ROBUST ADAPTIVE CONTROL OF MOBILE MANIPULATOR

Tan Lam Chung[(1)], Sang Bong Kim[(2)]
(1) National Key Lab of Digital Control and System Engineering, VNU-HCM
(2) Pukyong National University, Korea

ABSTRACT: *In this paper a robust control is applied to a two-wheeled mobile manipulator (WMM) to observe the dynamic behavior of the total system. To do so, the dynamic equation of the mobile manipulator is derived taking into account parametric uncertainties, external disturbances, and the dynamic interactions between the mobile platform and the manipulator; then, a robust controller is derived to compensate the uncertainty and disturbances solely based on the desired trajectory and sensory data of the joints and the mobile platform. Also, a combined system which composed of a computer and a multi-dropped PIC-based controller is developed using USB-CAN communication to meet the performance of demand of the whole system. What's more, the simulation and experimental results are included to illustrate the performance of the robust control strategy.*

Keywords: *robust adaptive controller, mobile manipulator*

1. INTRODUCTION

The design of intelligent, autonomous machines to perform tasks that are dull, repetitive, hazardous, or that require skill, strength, or dexterity beyond the capability of humans is the ultimate goal of robotics research. Examples of such tasks include manufacturing, excavation, construction, undersea, space, and planetary exploration, toxic waste cleanup, and robotic assisted surgery. Robotics research is highly interdisciplinary requiring the integration of control theory with mechanics, electronics, artificial intelligence, communication and sensor technology.

A mobile manipulator is of a manipulator mounted on a moving platform. Such the combined system has become an attraction of the researchers throughout the world. These systems, in one sense, considered to be as human body, so they can be applicable in many practical fields from industrial automation, public services to home entertainment.

In literature, a two-wheeled mobile robot has been much attracted attention because of its usefulness in many applications that need the mobility. Fierro, 1995, developed a combined kinematics and torque control law using backstepping approach and its asymptotic stability is guaranteed by Lyapunov theory which can be applied to the three basic nonholonomic navigations: trajectory tracking, path following and point stabilization [2]. Dong Kyoung Chwa et al., 2002, proposed a sliding mode controller for trajectory tracking of nonholonomic wheeled mobile robots presented in two-dimensional polar coordinates in the presence of the external disturbances [5]; T. Fukao, 2000, proposed the integration of a kinematic adaptive controller and a torque controller for the dynamic model of a nonholonomic mobile robot [4].

On the other hand, many of the fundamental theory problems in motion control of robot manipulators were solved. At the early stage, the major position control technique is known to be the computed torque control, or inverse dynamic control, which decouples each joint of the robot and linearizes it based on the estimated robot dynamic models; therefore, the performance of position control is mainly dependent upon the accurate estimations of robot dynamics. Spong and Vidyasaga [8] (1989) designed a controller based on the computed torque control for manipulators. The idea is to exactly compensate all of the coupling

nonlinearities in the Lagrangian dynamics in the first stage so that the second stage compensator can be designed based on linear and decoupling plant. Moreover, a number of techniques may be used in the second stage, such as, the method of stable factorization was applied to the robust feedback linearization problem [9] (1985). Corless and Leitmann [10] (1981) proposed a theory based on Lyapunov's second method to guaranty stability of uncertain system that can apply to the manipulators.

In this paper, a robust control based on the work of [11] was applied to two-wheeled mobile platform and a 6-dof manipulator taking into account parameter uncertainties and external disturbances. In [11], the controller was only applied to a two-link manipulator, and the platform is fixed. To design the tracking controller, the posture errors of the mobile platform and of the joints are defined, and the Lyapunov functions are defined for the two such subsystems and the whole system as well. The robust controllers are extracted from the bounded conditions of the parameters, disturbances and the sensory data of the mobile manipulator. Also, the simulation and experimental results show the effectiveness of the system model and the designed controllers. And this works was done in CIMEC Lab., Pukyong National University, Pusan, Korea.

2. DYNAMIC MODEL OF THE WMM

The model of the mobile manipulator is shown in Fig. 1.

First, consider a two-wheeled mobile platform which can move forward, and spin about its geometric center, as shown in Fig. 2. The length between the wheels of the mobile platform is $2b$ and the radius of the wheels is r_w. $\{OXY\}$ is the stationary coordinates system, or world coordinates system; $\{Pxy\}$ is the coordinates system fixed to the mobile robot, and P is placed in the middle of the driving wheel axis; $C(x_c, y_c)$ is the center of mass of the mobile platform and placed in the x-axis at a distance d from P; the length of the mobile platform in the direction perpendicular to the driving wheel axis is a and the width is L. It is assumed that the center of mass C and the origin of stationary coordinate P are coincided. The balance of the mobile platform is maintained by a small castor whose effect we shall ignore.

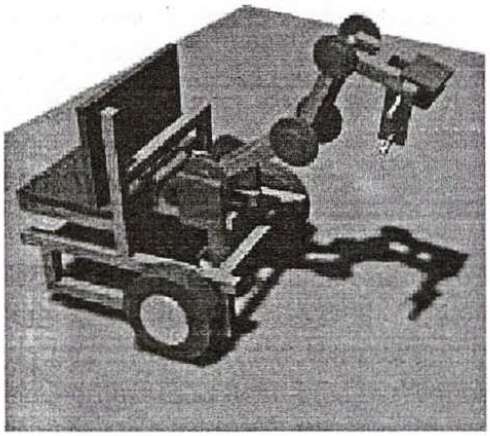

Fig 1. Model of the mobile manipulator

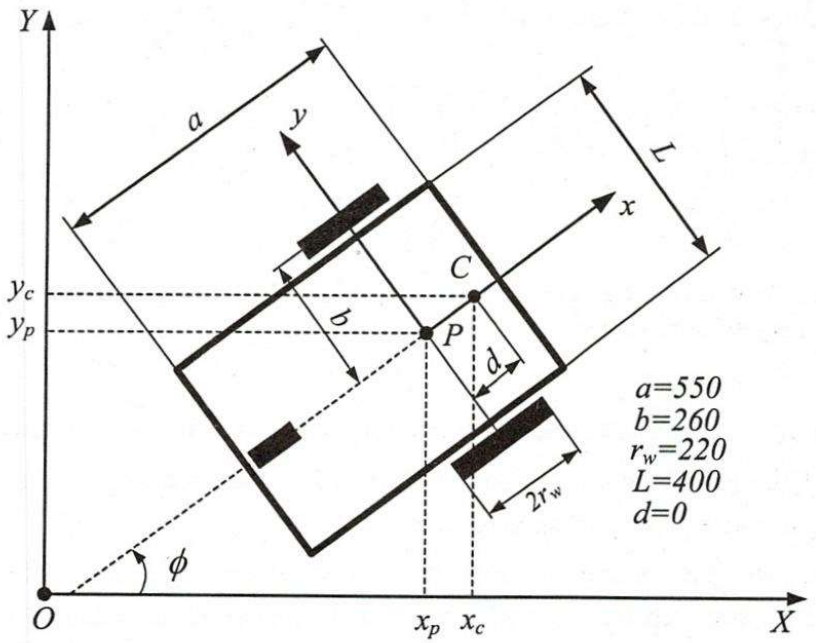

Fig 2. Mobile platform configuration

Second, the manipulator used in this application is of an articulated-type manipulator with two planar links in an elbow-like configuration: three rotational joints for three degrees of freedom. They are controlled by dedicated DC motors. Each joint is referred as the waist, shoulder and arm, respectively. Also, the manipulator has a 3-dof end-effector function as roll, pitch and yaw; and a parallel gripper attached to the yaw.

The length and the center of mass of each link are presented as (L_{b1}, Z_{b1}), (L_{b2}, Z_{b2}), (L_{b3}, Z_{b3}), (L_{b4}, Z_{b4}), (L_{b5}, Z_{b5}), respectively. The geometric model and the coordinate composed for each link is shown in Fig. 3.

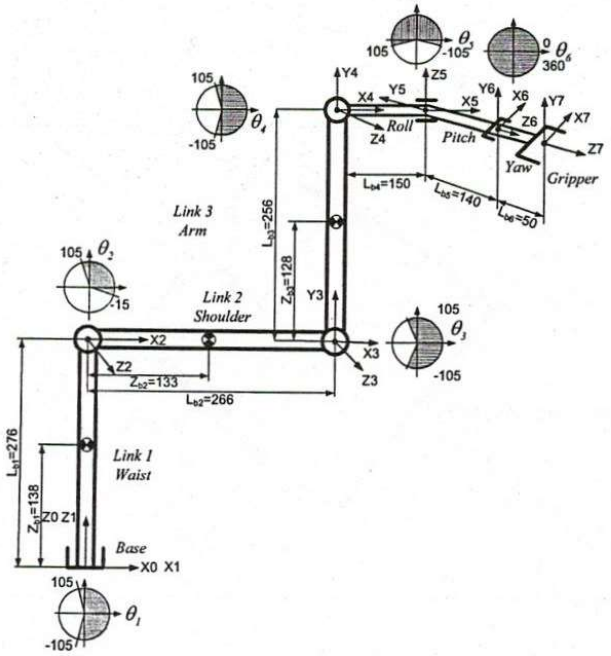

Fig 3. Geometry of 6-dof manipulator

The dynamics of the mobile manipulator subject to kinematics constraints is given in the following form [11]:

$$\begin{pmatrix} M_{11} & M_{12} \\ M_{21} & M_{22} \end{pmatrix}\begin{pmatrix} \ddot{q}_v \\ \ddot{q}_a \end{pmatrix}+\begin{pmatrix} C_{11} & C_{12} \\ C_{21} & C_{22} \end{pmatrix}\begin{pmatrix} \dot{q}_v \\ \dot{q}_a \end{pmatrix}+\begin{pmatrix} F_1 \\ F_2 \end{pmatrix}+\begin{pmatrix} A_v^T(q_v)\lambda \\ 0 \end{pmatrix}+ \begin{pmatrix} \tau_{d1} \\ \tau_{d2} \end{pmatrix}=\begin{pmatrix} E_v\tau_v \\ \tau_a \end{pmatrix} \quad (1)$$

The system constraint Eq. (1) can be simplified to the nonholonomic constraint of the mobile platform only as follows:

$$A_v(q_v)\dot{q}_v = 0 \quad (2)$$

where $\tau_v \in R^{m-r}$ represents the actuated torque vector of the constrained coordinates; $E_v \in R^{mx(m-r)}$, the input transformation matrix; $\tau_b \in R^n$, the actuating torque vector of the free coordinates; τ_{d1} and τ_{d2}, disturbance torques.

According to the standard matrix theory, there exists a full rank matrix $S_v(q_v) \in R^{mx(m-r)}$ made up by a set of smooth and linearly independent vector spanning the null space of A_v, that is, $S^T(q_v)A_v^T(q_v) = 0$. From Eq. (2), we can find a velocity input vector $\eta(t) \in R^{m-n}$ such that, for all t,

$$\dot{q}_v = S(q_v)\eta \quad (3)$$

The Eq. (3) is called the *steering system*, and η is known as a velocity input to steer the state vector q in state space. Furthermore, $S(q_v)$ is bounded by $S(q_v) \le \zeta_s$, ζ_s is a positive number.

2.1 Tracking Controller for the Mobile Platform

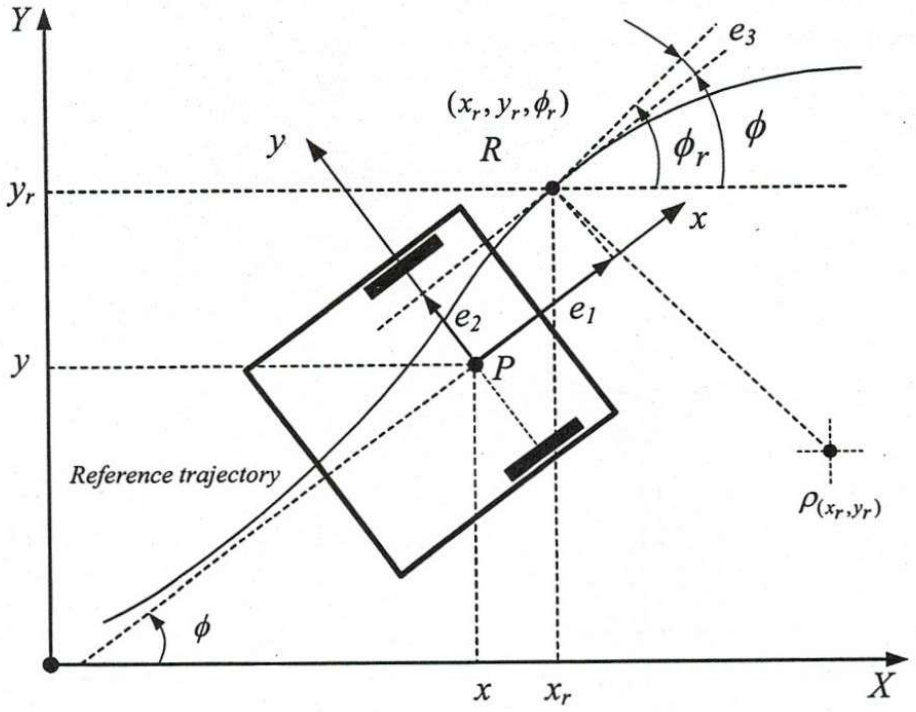

Fig 4. Kinematic analysis of tracking problem

The tracking errors of the mobile platform are given as follows [2]:

$$e=\begin{bmatrix} e_1 \\ e_2 \\ e_3 \end{bmatrix}=\begin{bmatrix} \cos\theta & \sin\theta & 0 \\ -\sin\theta & \cos\theta & 0 \\ 0 & 0 & 1 \end{bmatrix}\begin{bmatrix} x_r-x \\ y_r-y \\ \theta_r-\theta \end{bmatrix} \tag{4}$$

The first derivative of errors yields

$$\begin{bmatrix} \dot{e}_1 \\ \dot{e}_2 \\ \dot{e}_3 \end{bmatrix}=\begin{bmatrix} -1 & e_2 \\ 0 & -e_1 \\ 0 & -1 \end{bmatrix}\begin{bmatrix} v \\ \omega \end{bmatrix}+\begin{bmatrix} v_r\cos e_3 \\ v_r\sin e_3 \\ \omega_r \end{bmatrix} \tag{5}$$

The Lyapunov function is chosen as

$$V_0=\frac{1}{2}e_1^2+\frac{1}{2}e_2^2+\frac{1-\cos e_3}{k_2} \tag{6}$$

The derivative of V_0 can be derived as

$$\dot{V}_0=e_1(-v+v_r\cos e_3)+\frac{\sin e_3}{k_2}(\omega_r-\omega+k_2e_2v_r) \tag{7}$$

The velocity control law η_d achieves stable tracking of the mobile platform for the kinematic model as

$$\eta_d=\begin{bmatrix} v_d \\ \omega_d \end{bmatrix}=\begin{bmatrix} v_r\cos e_3+k_1e_1 \\ \omega_r+k_2v_re_2+k_3\sin e_3 \end{bmatrix} \tag{8}$$

Where k_1, k_2 and k_3 are positive values.

The Eq. (7) becomes

$$\dot{V}_0=-k_1e_1^2-\frac{k_3}{k_2}\sin^2 e_3 \tag{9}$$

Clearly $\dot{V}_1\le 0$ and the tracking errors $e=[e_1,e_2,e_3]^T$ is bounded along the system's solution. It is also assumed that not only the velocity of $v_r>0$ is constant with the orientation ϕ_r but also the reference angular velocity ω_r is bounded and have its bounded derivative for all t. From Eqs. (5), (6) and (9), it is shown that $\|e\|$ and $\|\dot{e}\|$ are bounded, so that $\ddot{V}_1<\infty$, that is, $\dot{V}_1$ is uniformly continuous. Since V_1 does not increase and converges to some constant value, by Barbalat's lemma, $\dot{V}_1\to 0$ as $t\to 0$. As $t\to\infty$, the limit of Eq. (9) becomes

$$0=k_1k_2e_1^2+k_3e_3^2 \tag{10}$$

Eq. (10) implies that $[e_1 \quad e_3]^T\to 0$ as $t\to\infty$.

From Eq. (5), the derivative of error e_3 is given

$$\dot{e}_3=\omega_r-\omega \tag{11}$$

Substituting ω in Eq. (11) by the kinematics control input ω_d in Eq. (8), the following result is derived

$$\dot{e}_3=-k_2e_2v_r-k_3\sin e_3 \tag{12}$$

Since $e_3\to 0$ as $t\to\infty$, the limit of Eq. (12) yields

$$\dot{e}_3=-k_2e_2v_r \tag{13}$$

Since $v_r^2 e_3$ has the limit equal to zero when $t \to \infty$, the derivative of this term can be derived as follows:

$$\frac{d}{dt}(v_r^2 e_3) = -k_2 v_r^2 e_2 \tag{14}$$

Since Eq. (14) is bounded, $v_r^2 e_2$ is uniformly continous. From Barbalat's lemma, $\frac{d}{dt}(v_r^2 e_3) = -k_2 v_r^2 e_2$ tends to zero. Therefore, $v_r^2 e_3$ tends to zero, and thus $v_r e_2$ tends to zero. Because the velocity of v_r is constant, $e_2 \to 0$ as $t \to \infty$ from Eq. (14). Hence, the equilibrium point $e = 0$ is *uniformly asymptotically stable.*

2.2 Lyapunov function for the mobile platform

Consider the first m-equation of Eq. (1) as follows:

$$M_{11}\ddot{q}_v + M_{12}\ddot{q}_a + C_{11}\dot{q}_v + C_{12}\dot{q}_a + F_1 + A_v^T \lambda + \tau_{d1} = E_v \tau_v \tag{15}$$

Multiplying both sides by S^T and using Eq. (3) to eliminate the constraint force term λ, it yields

$$M_{11}\dot{\eta} + \overline{C}_{11}\eta + f_1 + \overline{\tau}_{d1} = \overline{\tau}_v \tag{16}$$

Here $\overline{M}_{11} = S^T M_{11} S$, $\overline{C}_{11} = S^T C_{11} S + S^T M_{11} \dot{S}$, $f_1 = S^T (M_{12}\ddot{q}_a + C_{12}\dot{q}_a + F_1)$, $\overline{\tau}_{d_1} = S^T \tau_{d1}$, $\overline{\tau}_v = S^T E_v \tau_v$, and $S^T E_v = \begin{bmatrix} 1/r_w & 1/r_w \\ b/r_w & b/r_w \end{bmatrix}$

It can be seen that f_1, which consists of the gravitational and friction force vector F_1 and the dynamics interaction with the manipulator $(M_{12}\ddot{q}_a + C_{12}\dot{q}_a)$, and the disturbances on the mobile platform (terrain disturbance force) needs to be compensated online.

Property 1: $\dot{\overline{M}}_{11} - 2\overline{C}_{11}$ is skew-symmetric

Property 2: $\|\overline{M}_{11}\| = \|S^T M_{11} S\| \le \overline{M}_{11b}$ and $\|M_{12}\| \le M_{12b}$

Property 3: $\|\overline{C}_{11}\| = \|S^T C_{11} S\| \le \overline{C}_{11b}\|\dot{q}\|$ and $\|C_{12}\| \le C_{12b}\|\dot{q}\|$

Assumption 1: Disturbance on the mobile platform is bounded, that is, $\|\tau_{d1}\| \le \tau_{N1}$, with τ_{N1} is a positive constant.

Assumption 2: The friction and gravity on the mobile platform are bounded by $\|F_1(q_v, \dot{q}_v)\| \le \xi_0 + \xi_1\|\dot{q}\|$, where ξ_0 and ξ_1 representing some positive constants.

The *velocity tracking error* is defined as

$$\tilde{\eta} = \eta - \eta_d \tag{17}$$

then, the mobile platform dynamics in terms of velocity tracking error is derived as

$$\overline{M}_{11}\dot{\tilde{\eta}} + \overline{C}_{11}\tilde{\eta} + \overline{M}_{11}\dot{\eta}_d + \overline{C}_{11}\eta_d + f_1 + \overline{\tau}_{d1} = \overline{\tau}_v \tag{18}$$

Let us consider the following Lyapunov function

$$V_1 = \frac{1}{2}\tilde{\eta}^T \overline{M}_{11}\tilde{\eta} \tag{19}$$

and the derivative of V_1 can be derived as follows:

$$\dot{V}_1 = \tilde{\eta}^T(\bar{\tau}_v - \bar{M}_{11}\dot{\eta}_d - \bar{C}_{11}\eta_d - f_1 - \bar{\tau}_{d1}) \quad (20)$$

2.3 Lyapunov function of the manipulator

Consider the last n-equations of Eq. (1),

$$M_{22}\ddot{q}_a + C_{22}\dot{q}_a + (M_{21}\ddot{q}_v + C_{21}\dot{q}_v + F_2) + \tau_{d2} = \tau_a \quad (21)$$

Equation (21) represents the dynamic equation of the manipulator. In this equation, the unknown terms need to be compensated are the gravitational and friction force F_2, the dynamic interaction term $(M_{21}\ddot{q}_v + C_{21}\dot{q}_v)$, and the disturbances on the manipulator.

Property 4: $\dot{\bar{M}}_{22} - 2\bar{C}_{22}$ is skew-symmetric

Property 5: $\|M_{21}\| \le M_{21b}$ and $\|M_{22}\| \le M_{22b}$

Property 6: $\|C_{22}\| \le C_{22b}\|\dot{q}\|$ and $\|C_{21}\| \le C_{21b}\|\dot{q}\|$

Assumption 3: Disturbance on the manipulator is bounded, that is, $\|\tau_{d2}\| \le \tau_{N2}$, with τ_{N2} is a positive constant.

Assumption 4: Friction and gravity in Eq. (21) are bounded by $\|F_2(q,\dot{q})\| \le \xi_2 + \xi_3\|\dot{q}\|$, where ξ_2 and ξ_3 representing some positive constants.

The joint tracking error is defined, and its derivatives are derived as follows:

$$\begin{aligned} \tilde{q}_a &= q_{ad} - q_a \\ \dot{\tilde{q}}_a &= \dot{q}_{ad} - \dot{q}_a \end{aligned} \quad (22)$$

Also, the *filter tracking error* and its derivative,

$$\begin{aligned} r_a &= \dot{\tilde{q}}_a + k\tilde{q}_a, k = k^T > 0 \\ \dot{r}_a &= \ddot{\tilde{q}}_a + k\dot{\tilde{q}}_a = \ddot{q}_{ad} - \ddot{q}_a + k(r_a - k\tilde{q}_a) \end{aligned} \quad (23)$$

The manipulator dynamics equation can be formulated in terms of filtered tracking error as follows:

$$-M_{22}\dot{r}_a + (M_{22}k - C_{22})(r_a - k\tilde{q}_a) + f_2 + \tau_{d2} = \tau_a \quad (24)$$

where $f_2 = M_{22}\ddot{q}_{ad} + C_{22}\dot{q}_{ad} + (M_{21}\ddot{q}_v + C_{21}\dot{q}_v + F_2)$

The Lyapunov function for the manipulator is defined as

$$V_2 = \frac{1}{2} r_a^T M_{22} r_a \quad (25)$$

the time derivative of V_2 can be derived as follows

$$\begin{aligned} \dot{V}_2 &= r_a^T M_{22}\dot{r}_a + \frac{1}{2} r_a^T \dot{M}_{22} r_a \\ &= r_a^T[-\tau_a - (M_{22}k - C_{22})k\tilde{q}_a + M_{22}kr_a + f_2 + \tau_{d2}] \end{aligned} \quad (26)$$

2.4 Lyapunov function of the mobile manipulator

The Lyapunov function for the overall system, the mobile platform and the manipulator, can be defined and rearrange as follows:

$$
\begin{aligned}
V &= V_0 + \frac{1}{2}\begin{pmatrix} S\tilde{\eta} \\ -r_a \end{pmatrix}^T \begin{pmatrix} M_{11} & M_{12} \\ M_{12}^T & M_{22} \end{pmatrix} \begin{pmatrix} S\tilde{\eta} \\ -r_a \end{pmatrix} \\
&= V_0 + \frac{1}{2}(S\tilde{\eta})^T M_{11}(S\tilde{\eta}) - \frac{1}{2} r_a^T M_{12}^T (S\tilde{\eta}) - \frac{1}{2}(S\tilde{\eta})^T M_{12} r_a + \frac{1}{2} r_a^T M_{22} r_a \\
&= V_0 + \frac{1}{2}\tilde{\eta}^T (S^T M_{11} S)\tilde{\eta} - r_a^T M_{12}^T (S\tilde{\eta}) + \frac{1}{2} r_a^T M_{22} r_a \\
&= V_0 + \frac{1}{2}\tilde{\eta}^T \overline{M}_{11}\tilde{\eta} - r_a^T M_{12}^T (S\eta) + \frac{1}{2} r_a^T M_{22} r_a \\
&= V_0 + V_1 + V_2 - r_a^T M_{12}^T (S\tilde{\eta})
\end{aligned} \tag{27}
$$

Taking the time derivative of V yields

$$
\dot{V} = \dot{V}_0 + \dot{V}_1 + \dot{V}_2 - \frac{d}{dt}\left\{ r_a^T M_{21}(S\tilde{\eta}) \right\} \tag{28}
$$

Substituting (20), (26) into (28) yields

$$
\begin{aligned}
&\dot{V} = \dot{V}_0 + \tilde{\eta}^T (\bar{\tau}_v - \overline{M}_{11}\dot{\eta}_d - \overline{C}_{11}\eta_d - f_1 - \bar{\tau}_{d1}) \\
&+ r_a^T [-\tau_a - (M_{22}k - C_{22})k\tilde{q}_a + M_{22}kr_a + f_2 + \tau_{d2}] - \frac{d}{dt}\left\{ r_a^T M_{21}(S\tilde{\eta}) \right\}
\end{aligned} \tag{29}
$$

On the other hand, f_1 can be rewritten in terms of error tracking filter r_a as follows:

$$
\begin{aligned}
f_1 &= S^T (M_{12}\ddot{q}_a + C_{12}\dot{q}_a + F_1) \\
&= S^T \{M_{12}[\ddot{q}_{ad} - \dot{r}_a + k(r_a - k\tilde{q}_a)] + C_{12}[\dot{q}_{ad} - (r_a - k\tilde{q}_a)] + F_1\} \\
&= -S^T [M_{12}\dot{r}_a + (C_{12} - M_{12}k)(r_a - k\tilde{q}_a)] + S^T (M_{12}\ddot{q}_{ad} + C_{12}\dot{q}_{ad} + F_1) \\
&= -S^T [M_{12}\dot{r}_a + (C_{12} - M_{12}k)(r_a - k\tilde{q}_a)] + \bar{f}_1
\end{aligned} \tag{30}
$$

with $\bar{f}_1 = S^T (M_{12}\ddot{q}_{ad} + C_{12}\dot{q}_{ad} + F_1)$

Similarly, f_2, in terms of velocity error $\tilde{\eta}$ as follows:

$$
\begin{aligned}
f_2 &= M_{21}\ddot{q}_v + C_{21}\dot{q}_v + (M_{22}\ddot{q}_{ad} + C_{22}\dot{q}_{ad} + F_2) \\
&= M_{21}(\dot{S}\eta + S\dot{\eta}) + C_{21}S\eta + (M_{22}\ddot{q}_{ad} + C_{22}\dot{q}_{ad} + F_2) \\
&= (M_{21}S)\dot{\eta} + (M_{21}\dot{S} + C_{21}S)\eta + \bar{f}_2 \\
&= (M_{21}S)(\dot{\tilde{\eta}} + \dot{\eta}_d) + (M_{21}\dot{S} + C_{21}S)(\tilde{\eta} + \eta_d) + \bar{f}_2
\end{aligned} \tag{31}
$$

with $\bar{f}_2 = (M_{22}\ddot{q}_{ad} + C_{22}\dot{q}_{ad} + F_2)$

Substituting (30) and (31) into (29) yields

$$
\dot{V} = V_0 + \tilde{\eta}^T \{\bar{\tau}_v - \psi_1\} - \tilde{\eta}^T \bar{\tau}_{d1} + r_a^T \{-\tau_a + \psi_2\} + r_a^T \tau_{d2} \tag{32}
$$

where

$$
\psi_1 = \overline{M}_{11}\dot{\eta}_d + \overline{C}_{11}\dot{\eta}_d + \bar{f}_1 + S^T \{C_{12}k\tilde{q}_a + M_{12}k(r_a - k\tilde{q}_a)\}
$$

$$
\psi_2 = M_{22}kr_a + (C_{22} - M_{22}k)k\tilde{q}_a + \bar{f}_2 + M_{21}S\dot{\eta}_d + M_{21}\dot{S}\eta_d + C_{21}S\eta_d
$$

The nonlinear terms ψ_1 and ψ_2 are need to be identical online using robust control scheme in the following section based on the work in [14].

3. ROBUST CONTROLLER DESIGN

First, consider the second term of the Eq. (32) and using **Properties** (1)-(3) and **Assumptions** (1)-(2):

$$\begin{aligned}
&\tilde{\eta}^T\left\{\bar{\tau}_v-\bar{M}_{11}\dot{\eta}_d-\bar{C}_{11}\eta_d-\bar{f}_1-S^T\left[C_{12}k\tilde{q}_a+M_{12}k(r_a-k\tilde{q}_a)\right]\right\}-\tilde{\eta}^T\bar{\tau}_{d1}\\
&=\tilde{\eta}^T\bar{\tau}_v+\tilde{\eta}^T\begin{Bmatrix}-\bar{M}_{11}\dot{\eta}_d-S^TM_{12}\left[\ddot{q}_{ad}+k(r_a-k\tilde{q}_a)\right]-\bar{C}_{11}\eta_d-\\ S^TC_{12}\left[\dot{q}_{ad}+k\tilde{q}_a\right]-S^TF_1-S^T\tau_{d1}\end{Bmatrix}\\
&\le\tilde{\eta}^T\bar{\tau}_v+\tilde{\eta}^T\begin{Bmatrix}\left\|\bar{M}_{11}\right\|\left\|\dot{\eta}_d\right\|+S^T\left\|M_{12}\right\|\left\|\ddot{q}_{ad}+k(r_a-k\tilde{q}_a)\right\|+\\ \left\|\bar{C}_{11}\right\|\left\|\eta_d\right\|+S^T\left\|C_{12}\right\|\left\|\dot{q}_{ad}+k\tilde{q}_a\right\|+S^T\left\|F_1\right\|+S^T\left\|\tau_{d1}\right\|\end{Bmatrix}\\
&\le\tilde{\eta}^T\bar{\tau}_v+\left\|\tilde{\eta}\right\|\begin{Bmatrix}\bar{M}_{11b}\left\|\dot{\eta}_d\right\|+\varsigma_sM_{12b}\left\|\ddot{q}_{ad}+k(r_a-k\tilde{q}_a)\right\|+\bar{C}_{11b}\left\|\eta_d\right\|\left\|\dot{q}\right\|+\\ \varsigma_sC_{12b}\left\|\dot{q}_{ad}+k\tilde{q}_a\right\|\left\|\dot{q}\right\|+\varsigma_s(\xi_0+\xi_1\left\|\dot{q}\right\|+\tau_{N1})\end{Bmatrix}\\
&=\tilde{\eta}^T\bar{\tau}_v+\left\|\tilde{\eta}\right\|\Delta_1^T\varphi_1
\end{aligned}\tag{33}$$

where the unknown vector Δ_1^T and the robust damping vector φ_1 are defined in the following:

$$\begin{aligned}
&\Delta_1^T=(\bar{M}_{11b},\varsigma_sM_{12b},\bar{C}_{11b},\varsigma_sC_{12b},\xi_1\varsigma_s,(\xi_0+\tau_{N1})\varsigma_s)\\
&\varphi_1^T=(\left\|\dot{\eta}_d\right\|,\left\|\ddot{q}_{ad}+k(r_a-k\tilde{q}_a)\right\|,\left\|\eta_d\right\|\left\|\dot{q}\right\|,\left\|\dot{q}_{ad}+k\tilde{q}_a\right\|\left\|\dot{q}\right\|,\left\|\dot{q}\right\|,1)
\end{aligned}\tag{34}$$

Second, consider the third term of the Eq. (32) and using **Properties** (4)-(6) and **Assumptions** (3)-(4):

$$\begin{aligned}
&r_a^T\begin{bmatrix}-\tau_a+M_{22}kr_a+(C_{22}-M_{22}k)k\tilde{q}_a+\bar{f}_2+M_{21}S\dot{\eta}_d+\\ M_{21}\dot{S}\eta_d+C_{21}S\eta_d\end{bmatrix}+r_a^T\tau_{d2}\\
&\le-r_a^T\tau_a+r_a^T\begin{Bmatrix}M_{22}\left[\ddot{q}_{ad}+k(r_a-k\tilde{q}_a)\right]+M_{21}(S\dot{\eta}_d+\dot{S}\eta_d)+\\ C_{22}(\dot{q}_{ad}+k\tilde{q}_a)+C_{21}S\eta_d+F_2+\tau_{d2}\end{Bmatrix}\\
&\le-r_a^T\tau_a+r_a^T\begin{Bmatrix}\left\|M_{22}\right\|\left\|\ddot{q}_{ad}+k(r_a-k\tilde{q}_a)\right\|+\left\|M_{21}\right\|\left\|S\dot{\eta}_d+\dot{S}\eta_d\right\|+\\ \left\|C_{22}\right\|\left\|\dot{q}_{ad}+k\tilde{q}_a\right\|+\left\|C_{21}\right\|\left\|S\right\|\left\|\eta_d\right\|+\left\|F_2\right\|+\left\|\tau_{d2}\right\|\end{Bmatrix}\\
&\le-r_a^T\tau_a+\left\|r_a\right\|\begin{Bmatrix}M_{22b}\left\|\ddot{q}_{ad}+k(r_a-k\tilde{q}_a)\right\|+M_{21b}\left\|S\dot{\eta}_d+\dot{S}\eta_d\right\|+\\ C_{22b}\left\|\dot{q}_{ad}+k\tilde{q}_a\right\|\left\|\dot{q}\right\|+C_{21b}\varsigma_s\left\|\eta_d\right\|\left\|\dot{q}\right\|+\xi_2+\xi_3\left\|\dot{q}\right\|+\tau_{N2}\end{Bmatrix}\\
&=-r_a^T\tau_a+\left\|r_a\right\|\Delta_2^T\varphi_2
\end{aligned}\tag{35}$$

where the unknown vector Δ_2^T and the RDC vector φ_2 are defined as follows:

$$\begin{aligned}
&\Delta_2^T=(M_{22b},M_{12b},C_{22b},C_{12b}\varsigma_s,\xi_3,\xi_2+\tau_{N2})\\
&\varphi_2^T=(\left\|\ddot{q}_{ad}+k(r_a-k\tilde{q}_a)\right\|,\left\|S\dot{\eta}_d+\dot{S}\eta_d\right\|,\left\|\dot{q}_{ad}+k\tilde{q}_a\right\|\left\|\dot{q}\right\|,\left\|\eta_d\right\|\left\|\dot{q}\right\|,\left\|\dot{q}\right\|,1)
\end{aligned}$$

Let us choose the mobile platform and manipulator torque inputs as

$$\bar{\tau}_v=-k_{pv}\tilde{\eta}-k_{11}\tilde{\eta}\left\|\varphi_1\right\|^2\tag{36}$$

$$\tau_a=k_{pa}r_a+k_{22}r_a\left\|\varphi_2\right\|^2\tag{37}$$

where $k_{pv} \geq 0$, $k_{pa} \geq 0$, $k_{11} \geq 0$, and $k_{22} \geq 0$ are the controller gains; φ_1 and φ_2 are the robust damping control vectors, respectively. Then the tracking errors of the closed-loop system are guaranteed to be *globally uniformly ultimately bounded.*

Substituting (36) and (37) into (32) yields

$$
\begin{aligned}
\dot{V} &\leq -V_0 - k_{pv}\tilde{\eta}^T\tilde{\eta} - k_1\tilde{\eta}^T\tilde{\eta}\|\varphi_1\|^2 + \tilde{\eta}^T\Delta_1^T\varphi_1 - k_{pa}r_a^T r_a - k_2 r_a^T r_a\|\varphi_2\|^2 + \|r_a\|\Delta_2^T\varphi_2 \\
&\leq -V_0 - k_1\|\eta_d\|^2\|\varphi_1\|^2 + \|\eta_d\|\|\Delta_1\|\|\varphi_1\| - k_2\|r_a\|^2\|\varphi_2\|^2 + \|r_a\|\|\Delta_2\|\|\varphi_2\| \\
&= -V_0 - k_1\left(\|\eta_d\|^2\|\varphi_1\|^2 - \frac{\|\eta_d\|\|\Delta_1\|\|\varphi_1\|}{k_1}\right) - k_2\left(\|r_a\|^2\|\varphi_2\|^2 - \frac{\|r_a\|\|\Delta_2\|\|\varphi_2\|}{k_2}\right) \\
&= -V_0 - k_1\left[\left(\|\eta_d\|\|\varphi_1\| - \frac{\|\Delta_1\|}{2k_1}\right)^2 - \frac{\|\Delta_1\|^2}{4k_1^2}\right] - k_2\left[\left(\|r_a\|\|\varphi_2\| - \frac{\|\Delta_2\|}{2k_2}\right)^2 - \frac{\|\Delta_2\|^2}{4k_2^2}\right] \\
&= -V_0 - k_1\left[\left(\|\eta_d\|\|\varphi_1\| - \frac{\|\Delta_1\|}{2k_1}\right)^2\right] - k_2\left[\left(\|r_a\|\|\varphi_2\| - \frac{\|\Delta_2\|}{2k_2}\right)^2\right] + \frac{\|\Delta_1\|^2}{4k_1} + \frac{\|\Delta_2\|^2}{4k_2} \\
&< -k_{\min}\left\{\left(\|\eta_d\|\|\varphi_1\| - \frac{\|\Delta_1\|}{2k_1}\right)^2 + \left(\|r_a\|\|\varphi_2\| - \frac{\|\Delta_2\|}{2k_2}\right)^2\right\} + \frac{\delta_{\max}^2}{2k_{\min}}
\end{aligned}
\tag{38}
$$

where $k_{\min} = \min\{k_1, k_2\}$ and $\delta_{\max} = \max\{\|\Delta_1\|, \|\Delta_2\|\}$

In Eq. (38), $\delta_{\max}$ is a bounded quantity; therefore, V decreases monotonically until the solutions reach a compact set determined by the right-hand-side of Eq. (32). The size of the residual set can be decreased by increasing $k_{\min}$. According to the standard Lyapunov theory and the extension of the LaSalle theory, this demonstrates that the control input Eqs. (36) and (37) can guarantee global uniform ultimate boundedness of all tracking errors.

Block diagram of robust controller is shown in Fig. 5

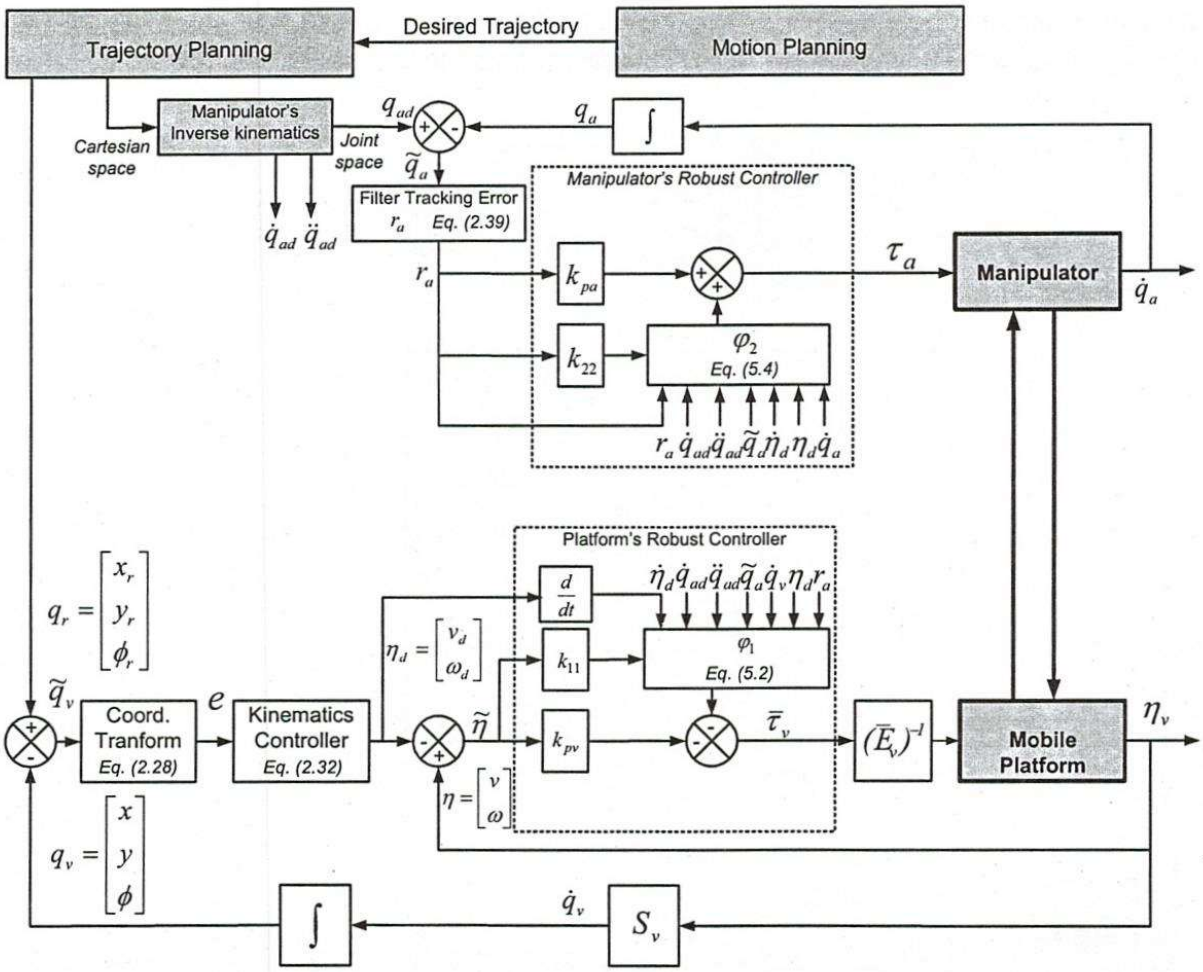

Fig 5. Block diagram of robust controller

4. CONTROL SYSTEM DEVELOPMENT

The control system is based on the integration of computer and PIC-based microprocessor. The computer functions as high as high level control for image processing (not presented in this paper) and control algorithm and the microprocessor, as low level controller for device control. The configuration diagram of the overall control system is shown in Fig. 6. In the configuration, there are 8 Servo-CAN modules are used to control all low-level devices: waist motor, shoulder motor, arm motor, roll motor, pitch motor, and yaw motor for manipulator; and left-wheeled and right-wheeled motors for mobile platform. The positions of the manipulator's joints feedback to the computer via ADC module on USB-CAN. The Servo-CAN module is based on PIC18F458 shown in Fig. 8. The USB-CAN module is used to interface between high and low levels: it transforms the serial data from computer to CAN messages shown in Fig. 7. The USB-CAN interface is shown in Fig. 9.

For the operation, USB camera Logitech 4000 is used to capture the image stream into memory with size of 320x240 at 30fps using QuickCam SDK. The image is processed using image processing library OpenCV to extract the features from the image for the object's position detection. The torque command is sent to the low level to control the mobile platform and the manipulator to perform a certain task. The total control processes are programmed and

integrated into the interface IMR V.1 in Visual C++ shown in Fig. 10. With this interface, the mobile manipulator's parameters can be set before the operation.

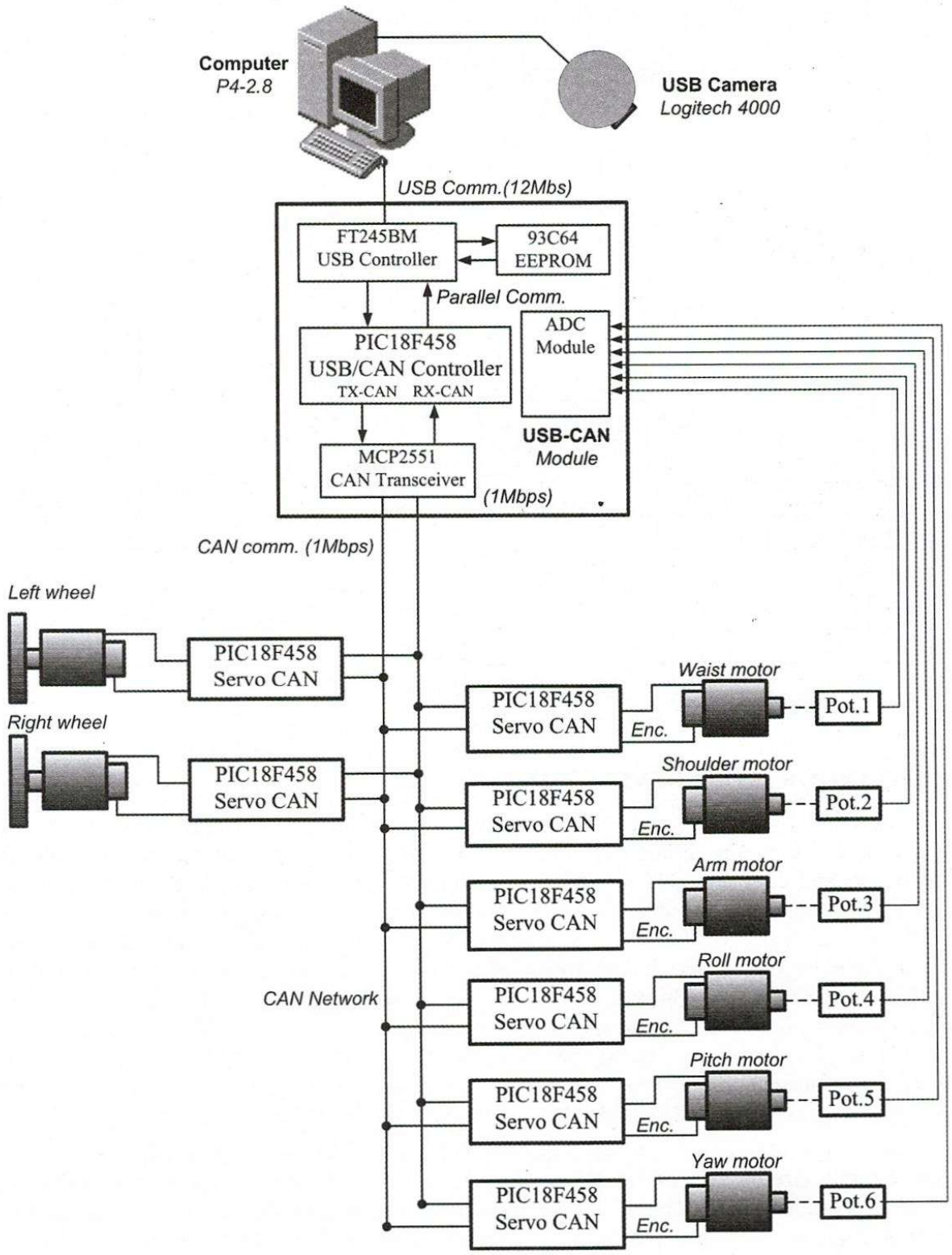

Fig 6. Diagram of the control system

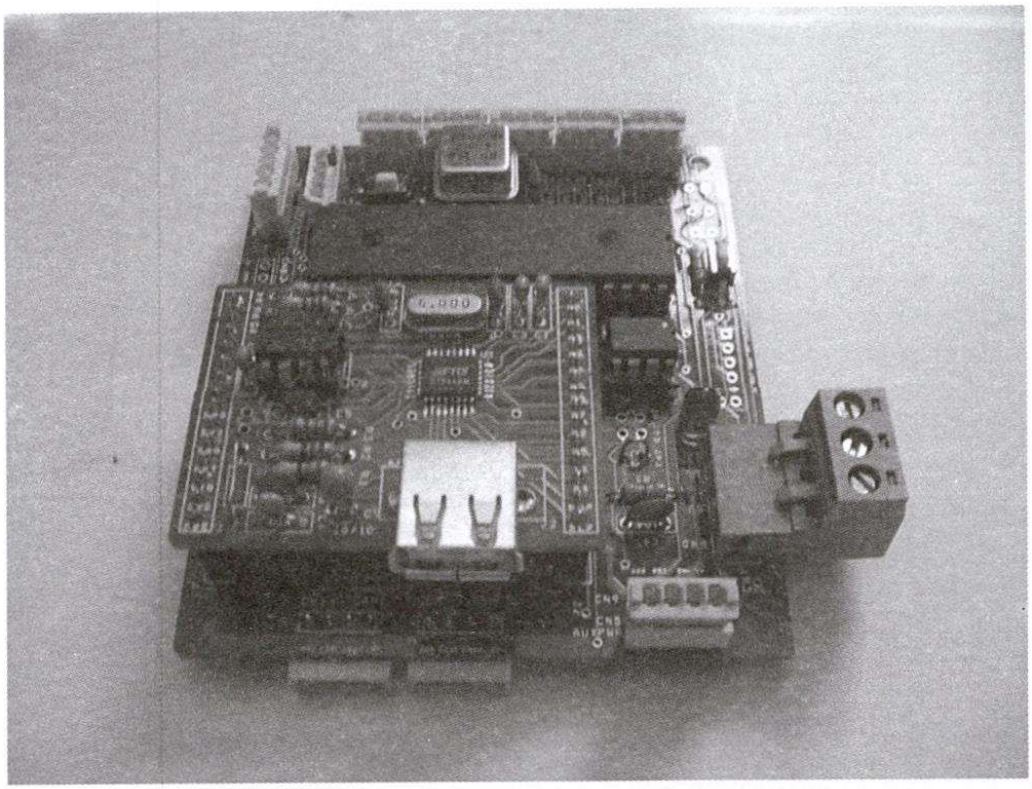

Fig 7. USB-CAN module

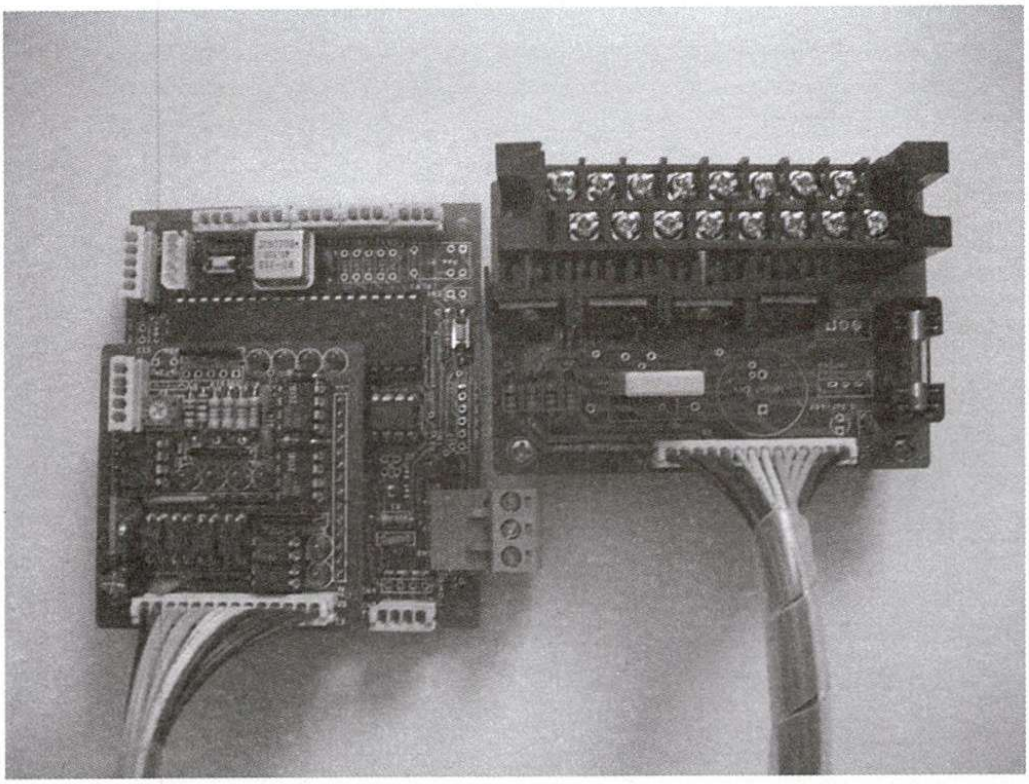

Fig 8. Servo CAN module

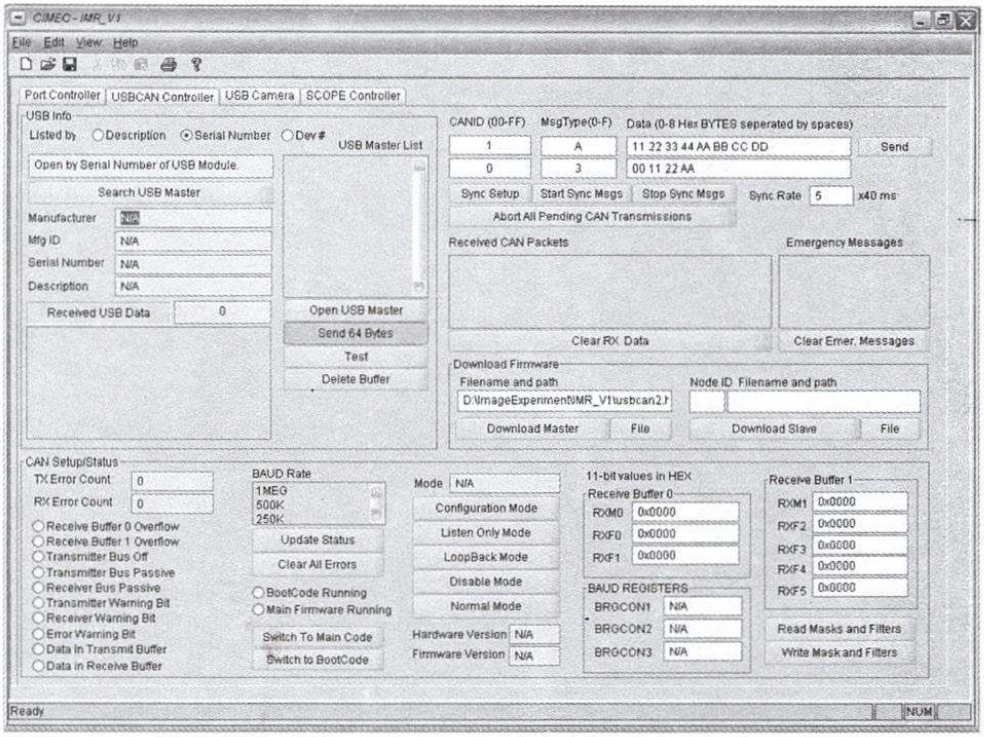

Fig 9. USB-CAN Interface

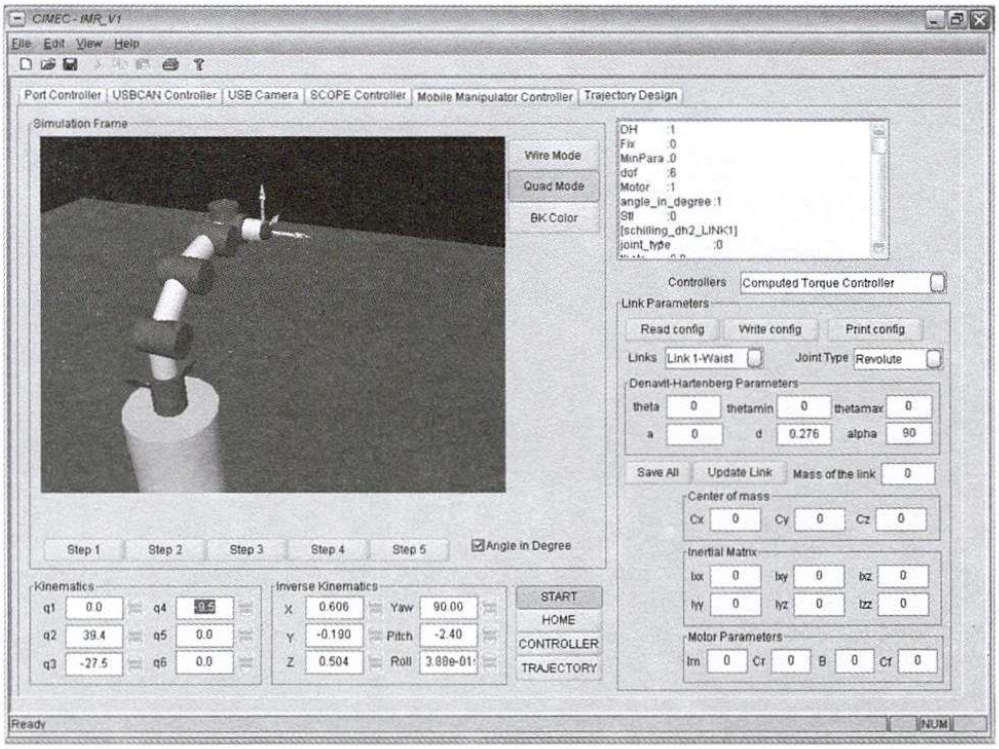

Fig 10. Mobile manipulator interface IMR V.1

5. SIMULATION RESULTS

To verify the effectiveness of the controller, the simulations have been done with controller (8),(36) and (37) using Visual C++6 (with matrix package) and Gnuplot 4. The reference trajectory are planned for the total system: a cubic spline reference line for the mobile platform shown in Fig. 11 with the trajectory parameters in Fig. 12 and sinusoid trajectory for joint 1 to joint 6 with the frequency of $0.8f, 0.9f, f, 1.1f, 1.2f$ and $1.3f$ ($f = 0.3125Hz$) as shown in Fig. 21, respectively. The kinematic controller constants are $k1 = 5, k_2 = 20$ and $k_3 = 10$. The robust controller gains are $k_{pv} = 40, k_{11} = 0.001, k_{pa} = 300, k_{22} = 1.2$. The mobile robot for the simulation has the following parameters: $b = 200mm$, $r = 110mm$, $m_c = 20.6kg$, $m_w = 1.2kg$. The initial posture of the mobile manipulator and the reference trajectory is $x(0) = 0.1m$, $y(0) = 0.3m$, $\phi(0) = 45^\circ$, $x_r(0) = 0.3m$, $y_r(0) = 0.5m$, $\phi_r(0) = 0$, respectively; the initial joint positions, $q_a(0) = (\pi/6, \pi/10, \pi/18, -\pi/18, -\pi/10, -\pi/6)$. Sampling time is 10ms. The disturbance is a random noise with the magnitude of 3, but it is not considered in this simulation.

Simulation results are given through Figs. 13-29. The mobile platform's tracking errors are given in Fig. 13 for full time (8s) and Fig. 12 for the initial time (2s), respectively. It can be seen that the platform errors go to zero after about 1 second. The kinematics control input, the linear and angular velocities at mobile platform center, is shown in Fig. 15; the velocities of the left and right wheel, in Fig. 16. It can be seen that the tracking velocity is in the vicinity of 2m/s as desired, but it should be tuned for the acceptable value in the practical applications. The robust vector for the mobile platform $\varphi_1 (i = 1..6)$ in the controller Eq. (36) is given in Fig. 17, and the torque on the left and the right wheel, in Fig, 18. The mobile platform's tracking position with respect to the reference trajectory is shown in Fig. 19 for the initial time (2s) and in Fig. 20 for full time (8s). As for the manipulator, the tracking positions of joint 1 to joint 6 are shown in Figs. 22-27. It can be seen that the overall tracking performance is acceptable, but they each are depend on the frequency of the reference trajectory. The joint's position errors and joint's torques are shown in Figs. 28 and 29, respectively.

The experimental results are given through Figs. 30-39. The reference trajectory for the experiment is designed again to be satisfied the mechanical condition of the experimental mobile manipulator. The reference trajectory of the platform is given in Fig. 30. The posture of the mobile platform can be calculated using dead-reckoning method via encoders, then the errors e_1, e_2 and e_3 can be derived shown in Figs. 31- 33. The errors go to zero after about 3 seconds. The joint's reference trajectory for the manipulator is designed as sinusoidal trajectory with slower frequencies than those in the simulation, that is, $0.8f, 0.9f, f, 1.1f, 1.2f$ and $1.3f$ ($f = 0.25Hz$). The joint's position errors are shown in Figs. 34-39, respectively; they are satisfied the tracking performance in the manner of ordinary applications.

Overall, the simulation and experimental results are reasonably same; it can be concluded that the kinematics controller and the robust controller are all applicable for practical fields. The experimental test bed is shown in Fig. 40.

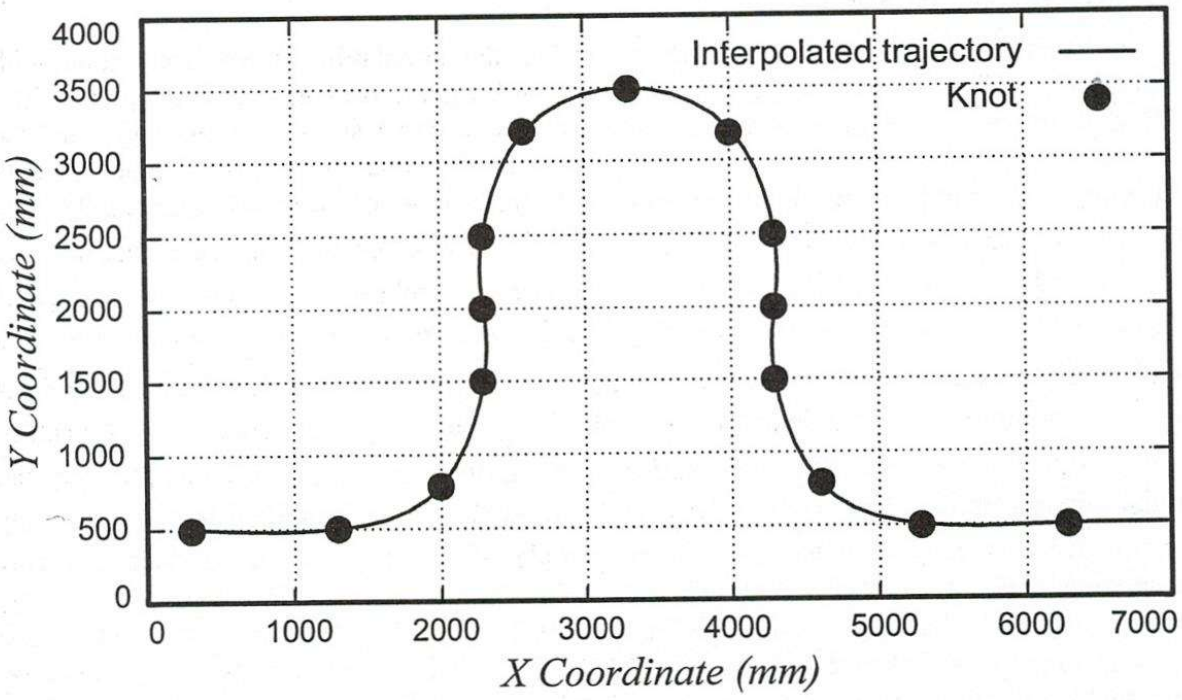

Fig 11. Cubic spline reference trajectory for platform

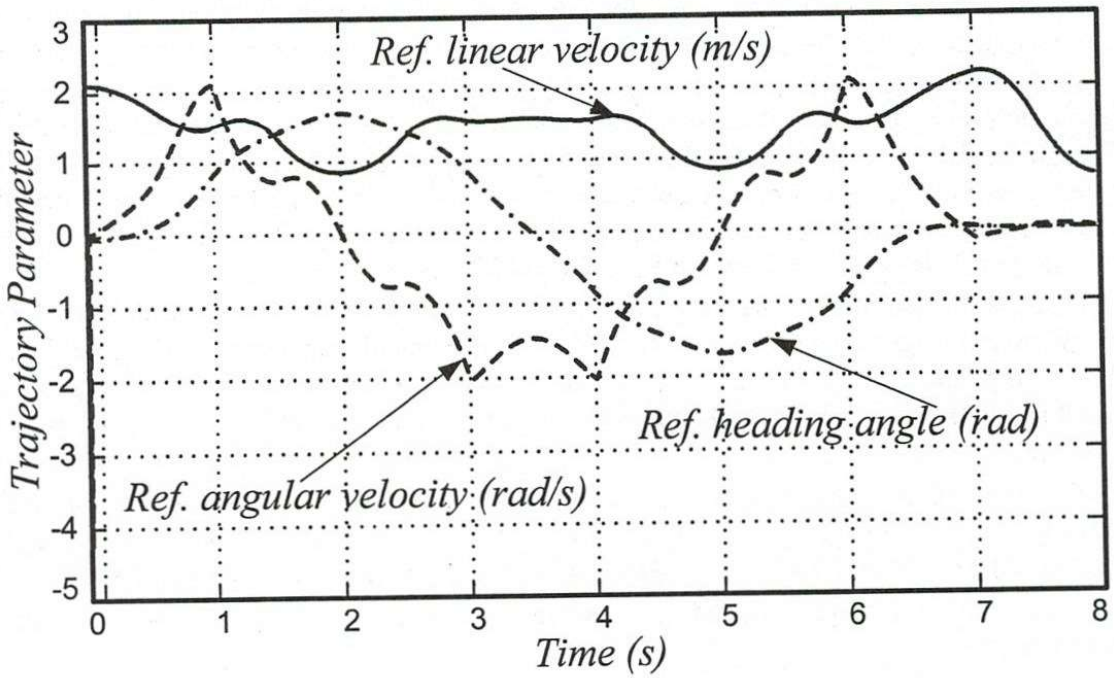

Fig 12. Reference trajectory parameters for platform

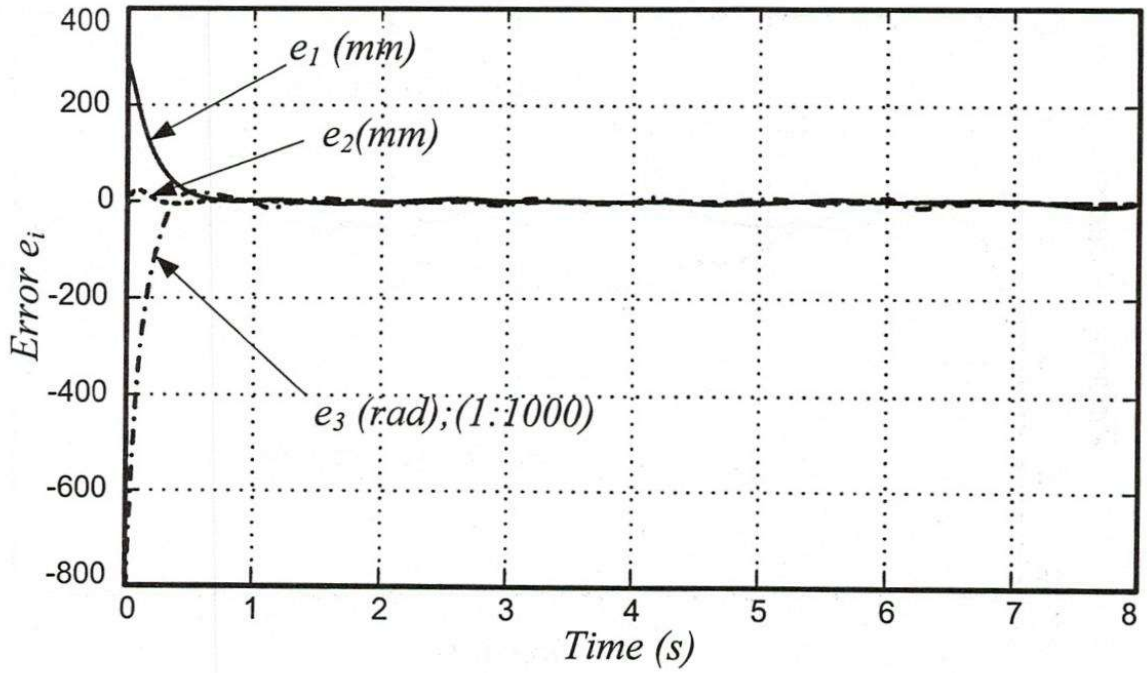

Fig 13. Platform tracking errors for full time

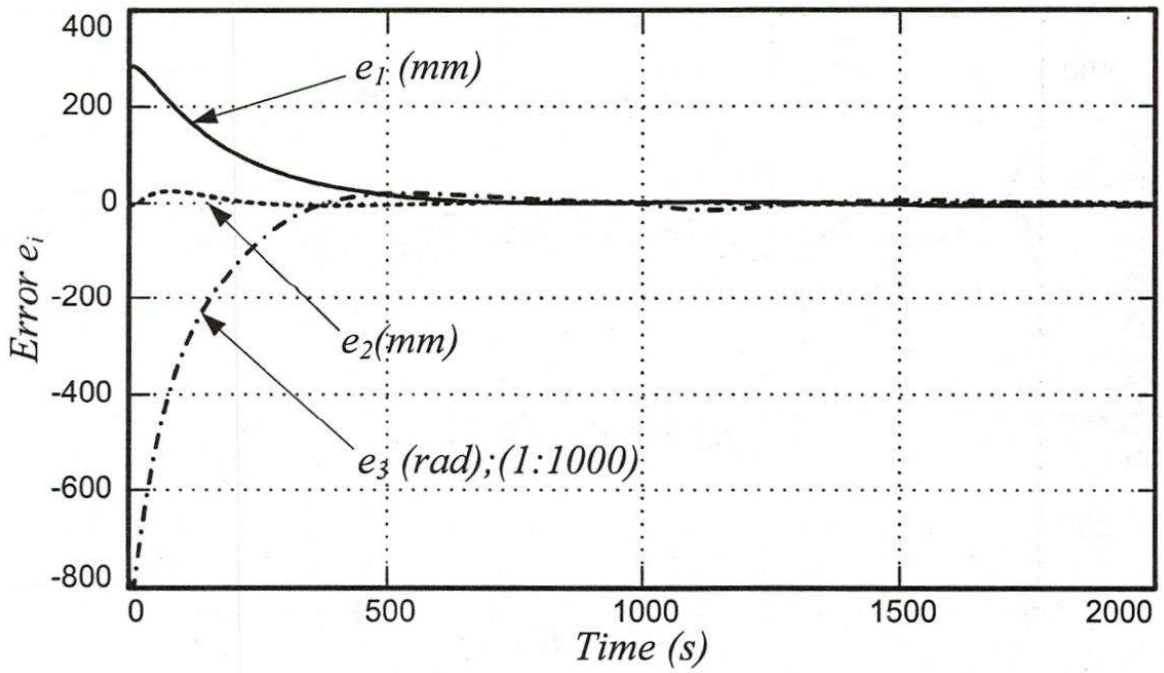

Fig 14. Platform tracking errors for the initial time

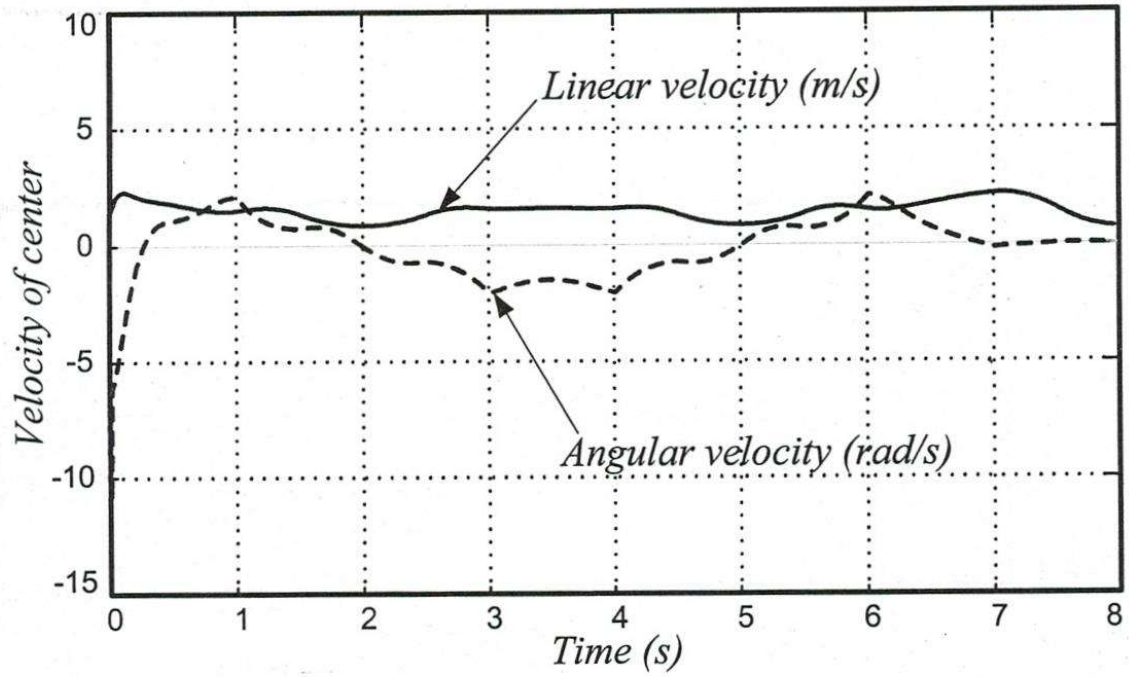

Fig 15. Velocities of platform's center

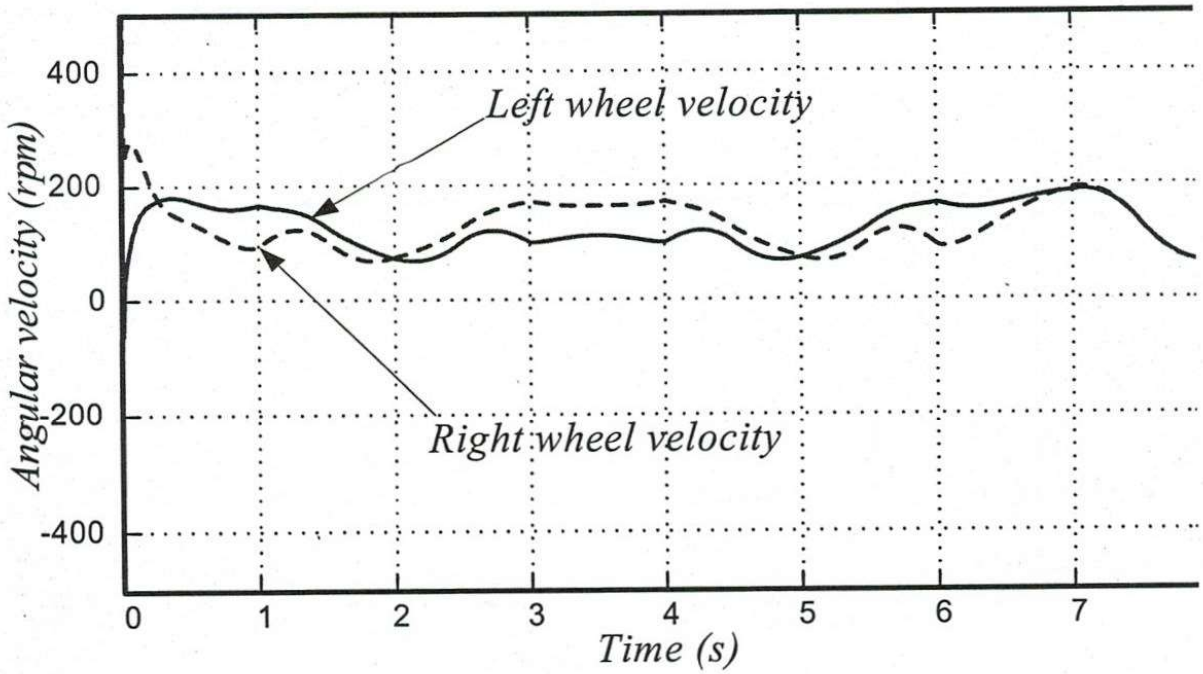

Fig 16. Wheel velocities

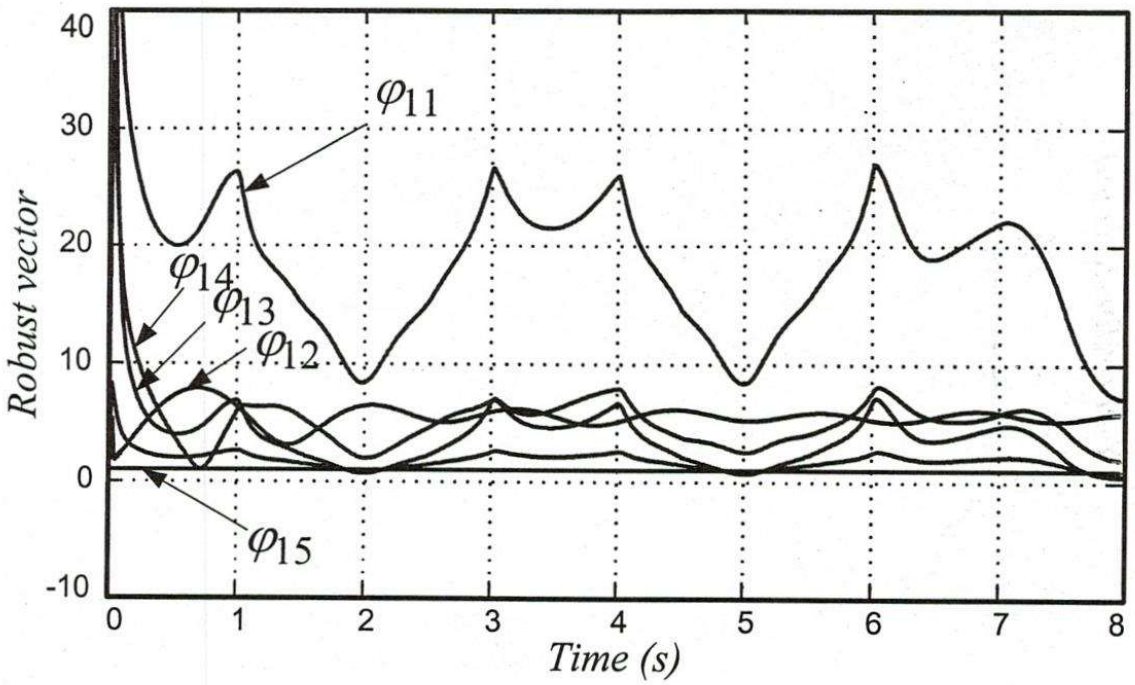

Fig 17. Robust vector of mobile platform

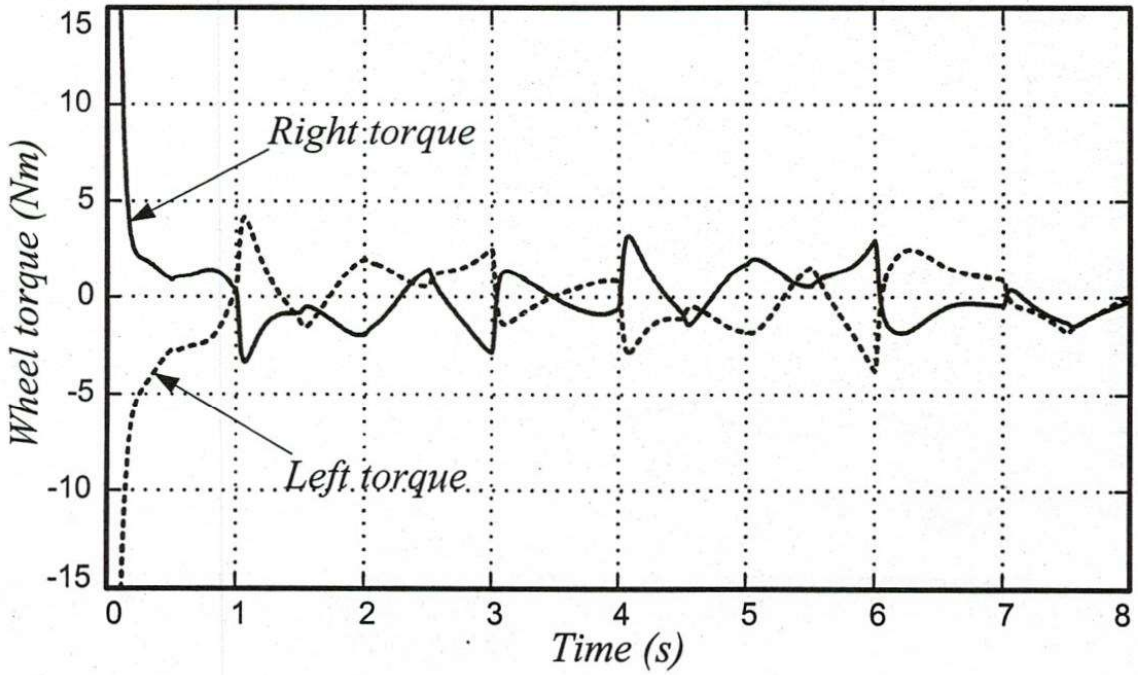

Fig 18. Wheel's torques of mobile platform

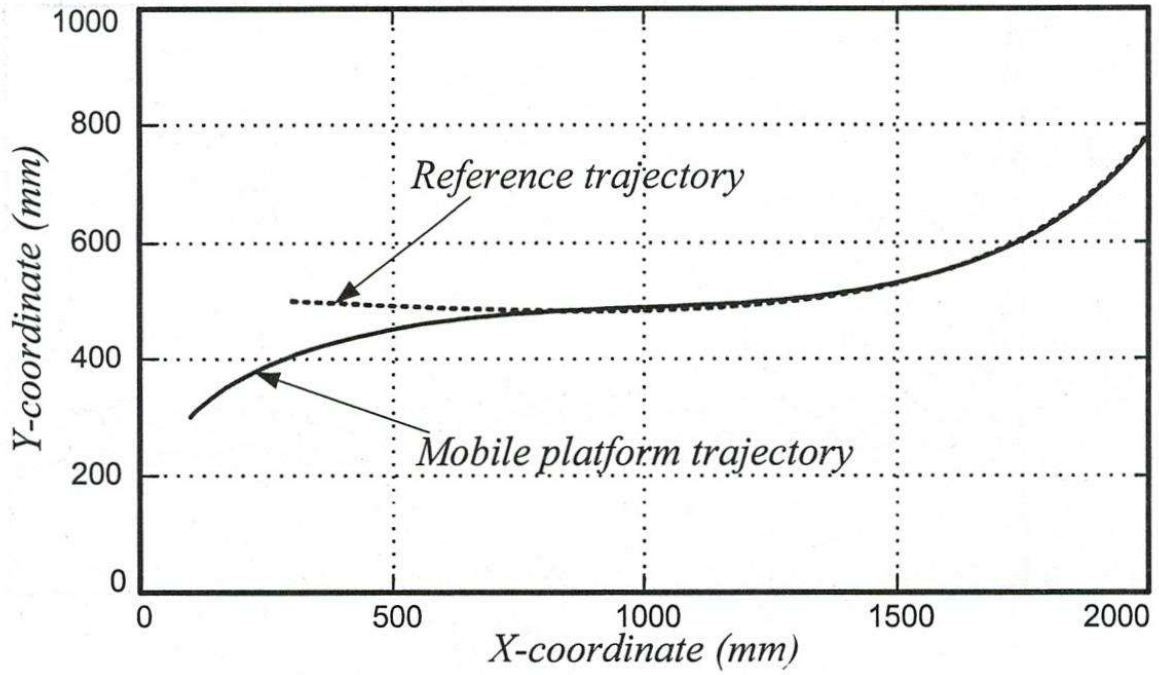

Fig 19. Tracking trajectory of mobile platform (2s)

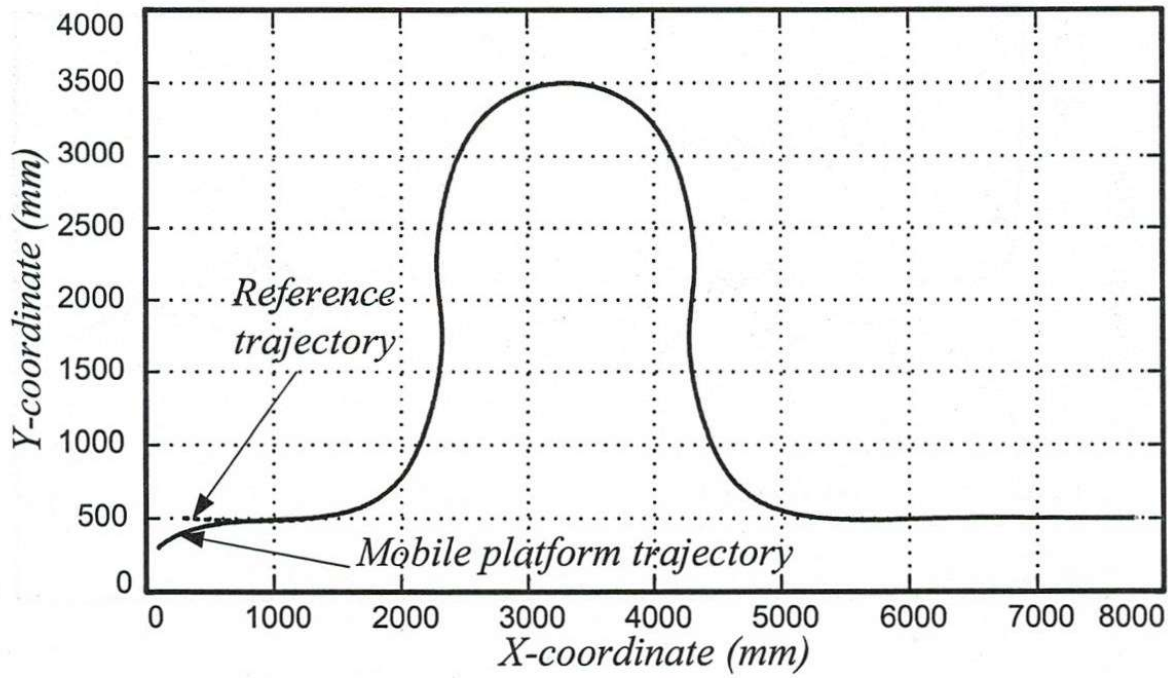

Fig 20. Tracking trajectory of mobile platform (8s)

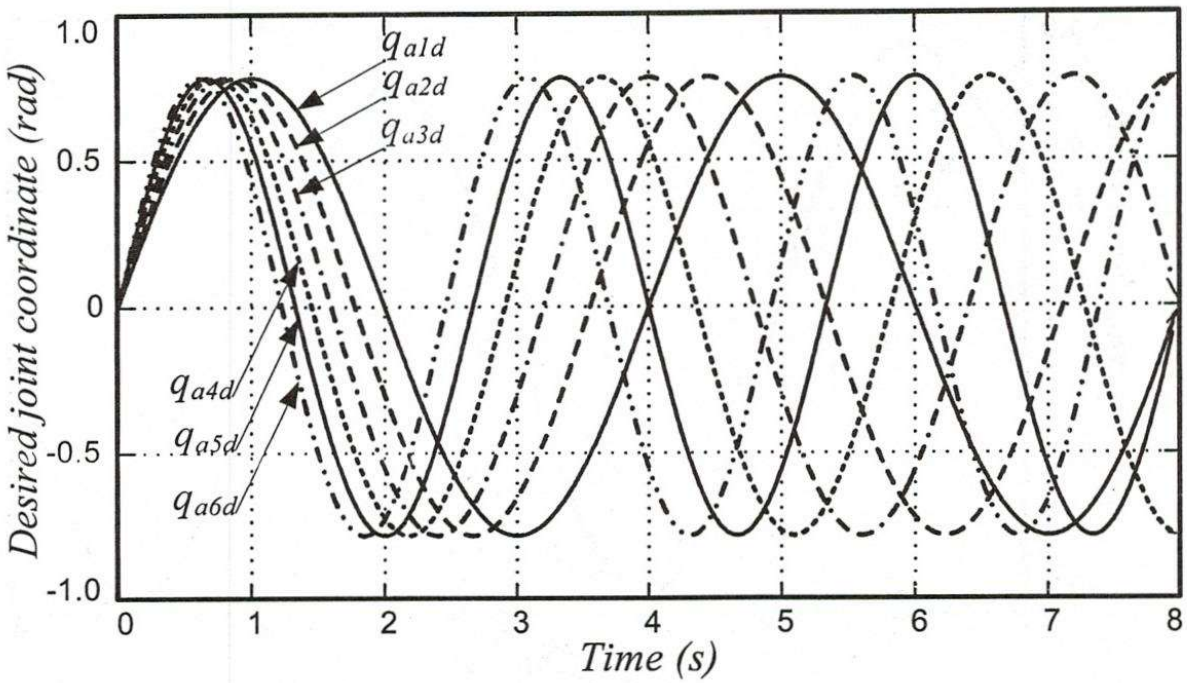

Fig 21. Joint reference trajectory

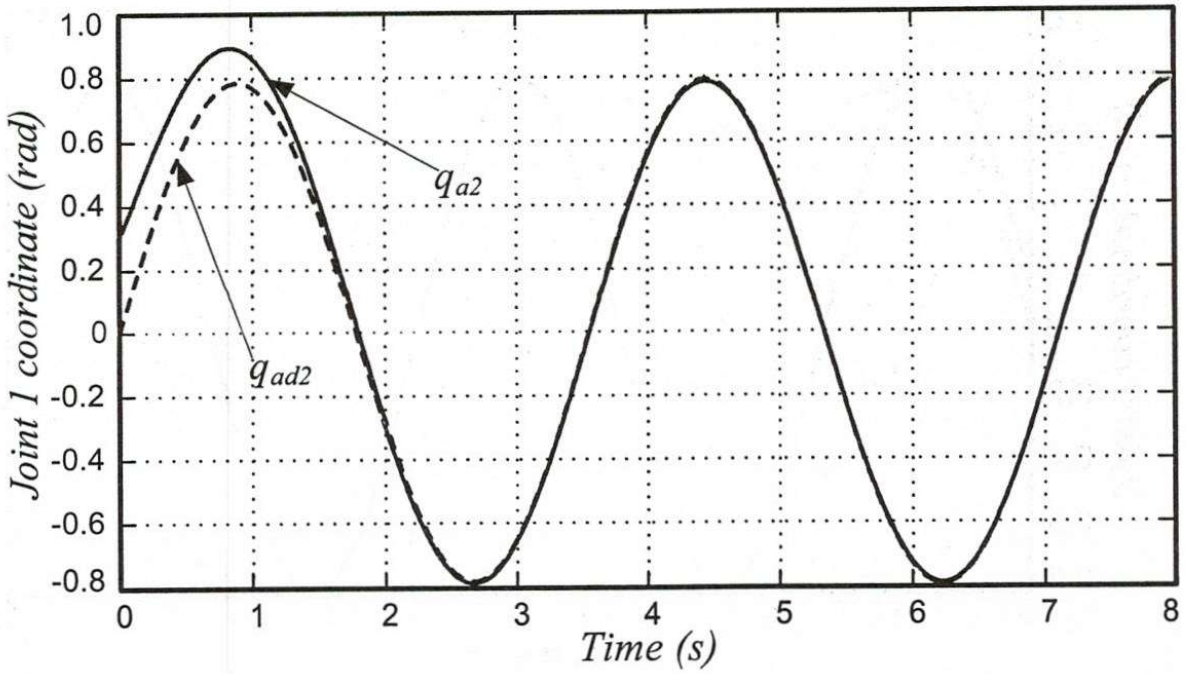

Fig 22. Tracking position of joint 1

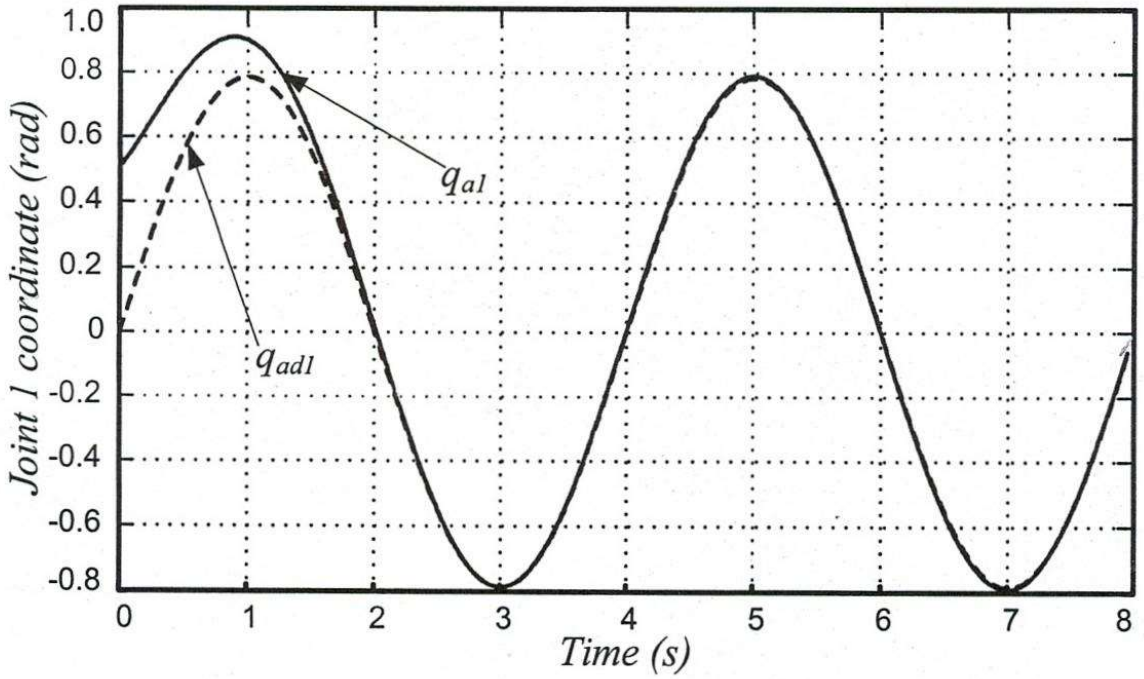

Fig 23. Tracking position of joint 2

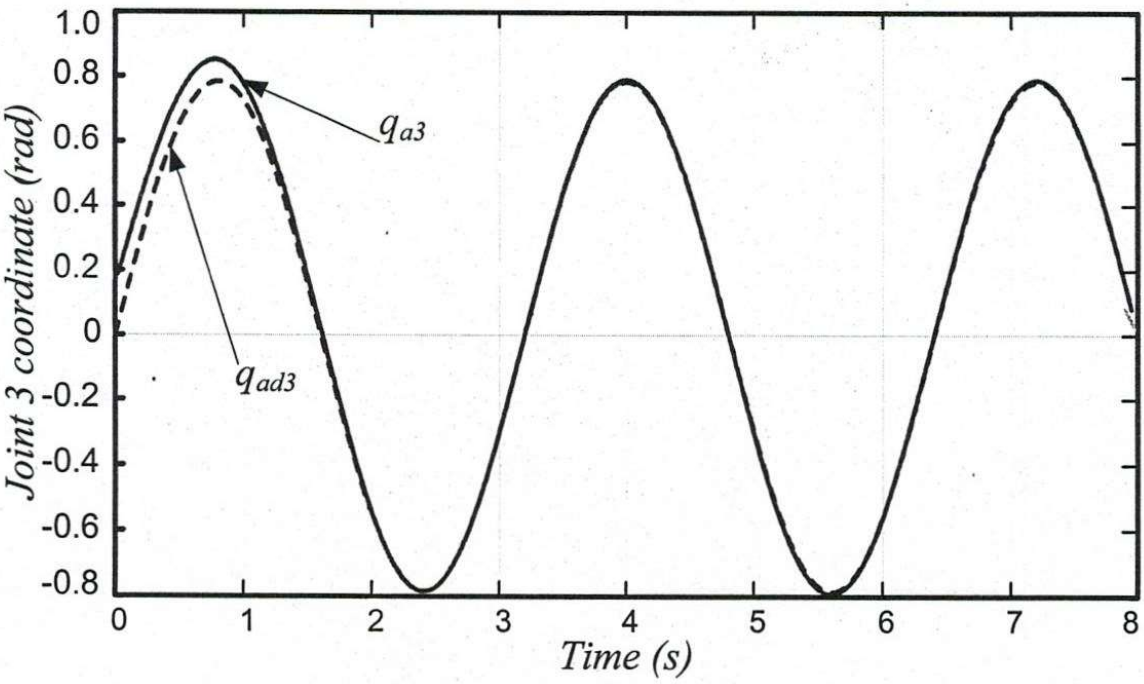

Fig 24. Tracking position of joint 3

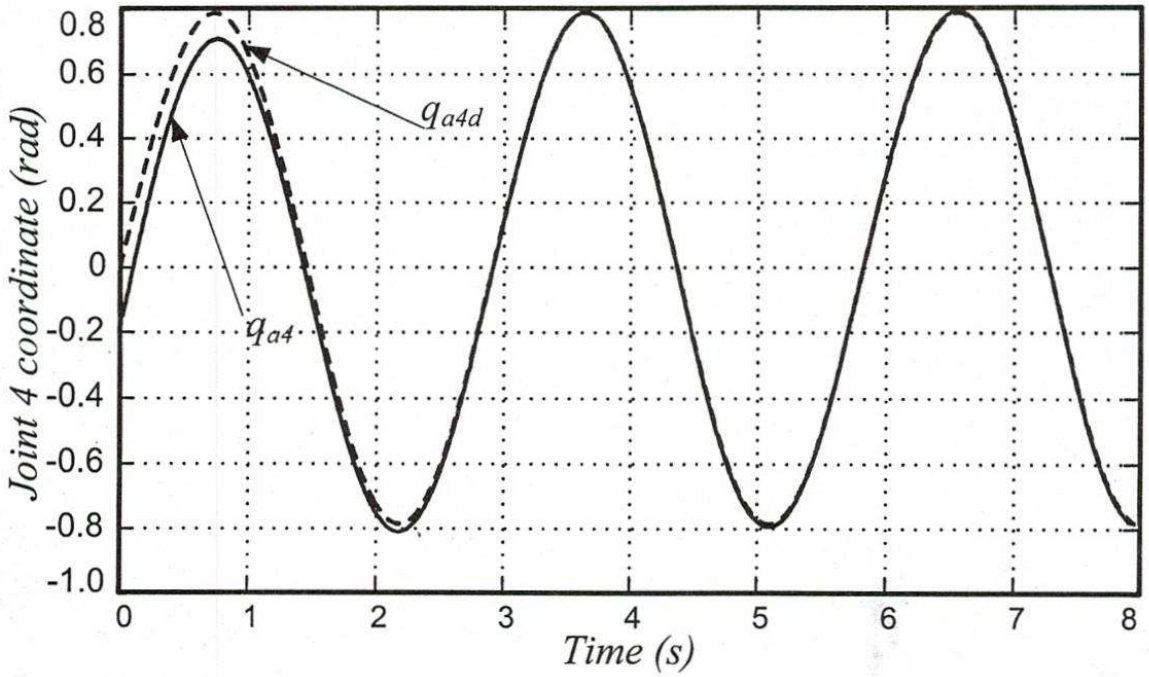

Fig 25. Tracking position of joint 4

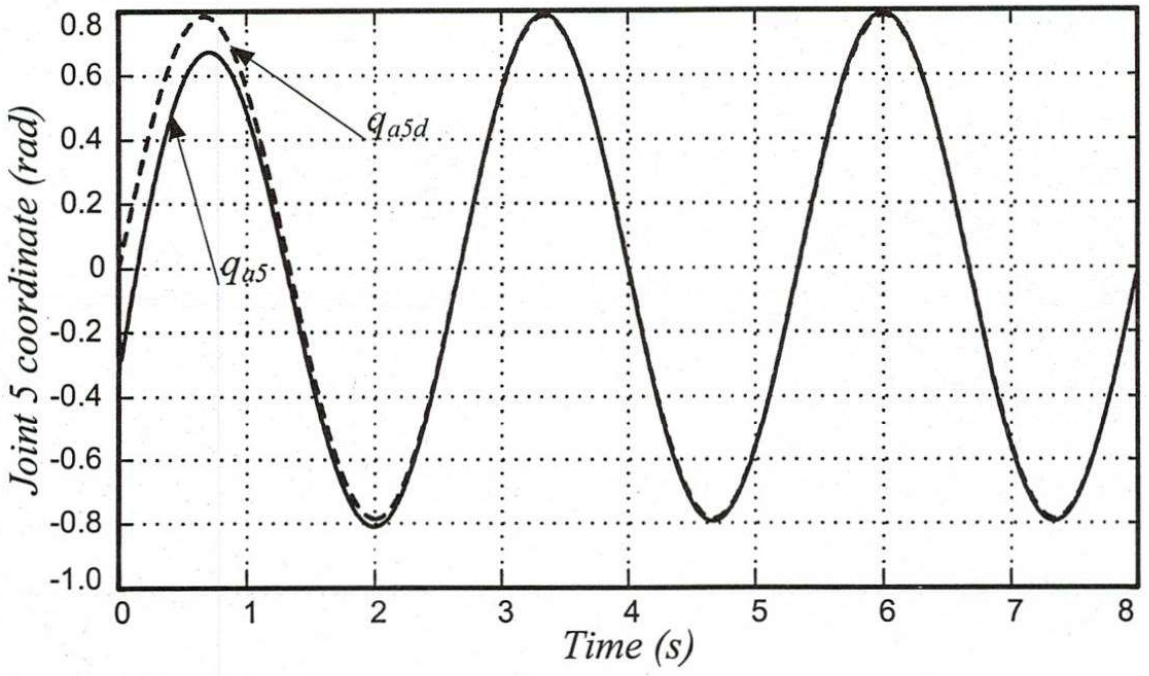

Fig 26. Tracking position of joint 5

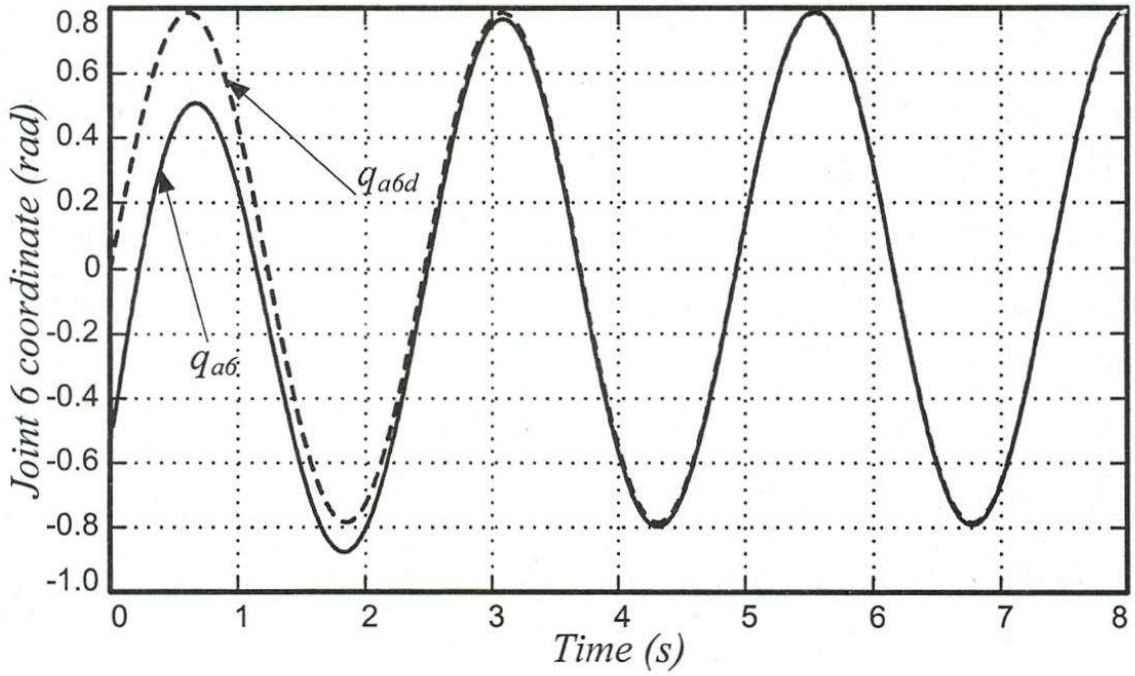

Fig 27. Tracking position of joint 6

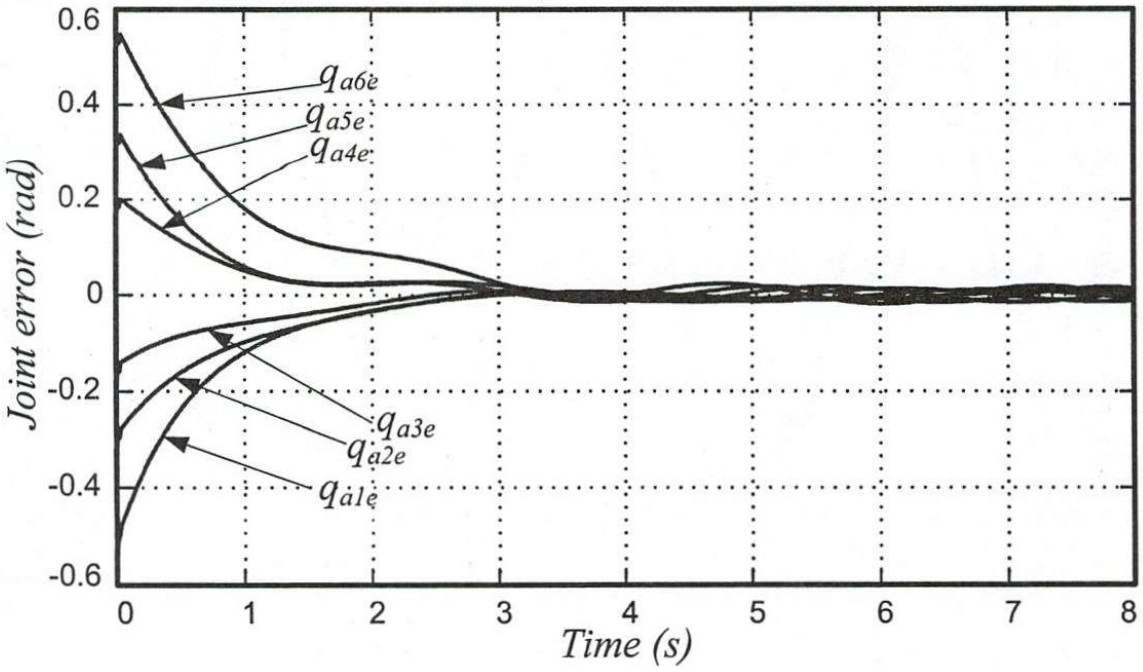

Fig 28. Joint position error

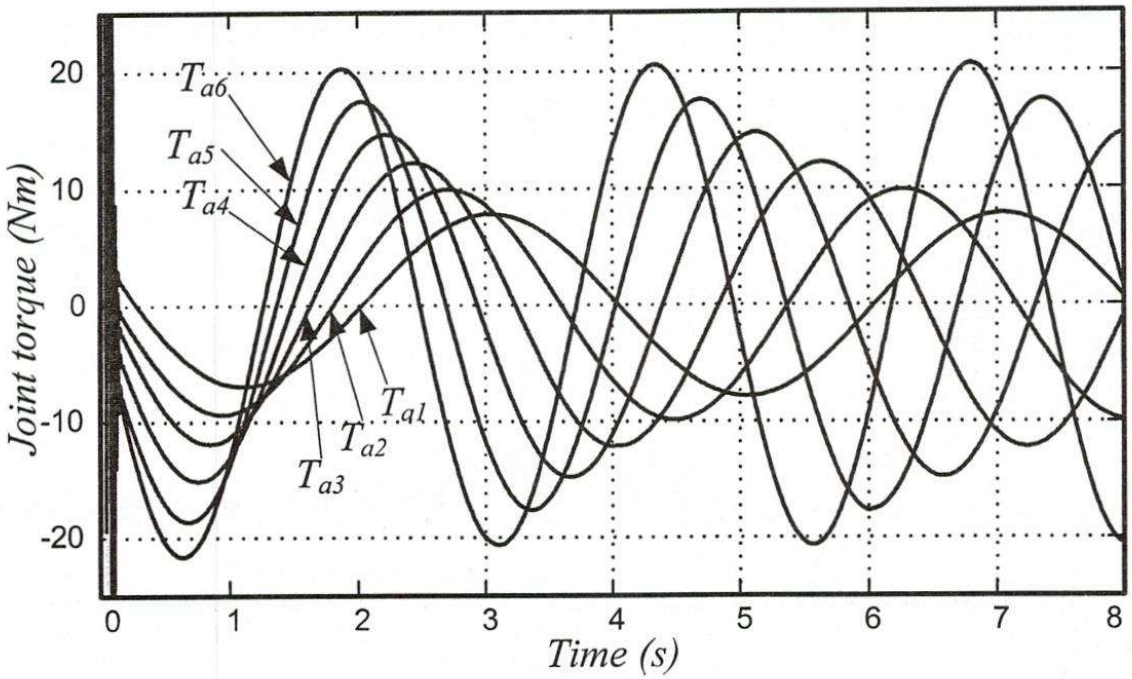

Fig 29. Joint torque

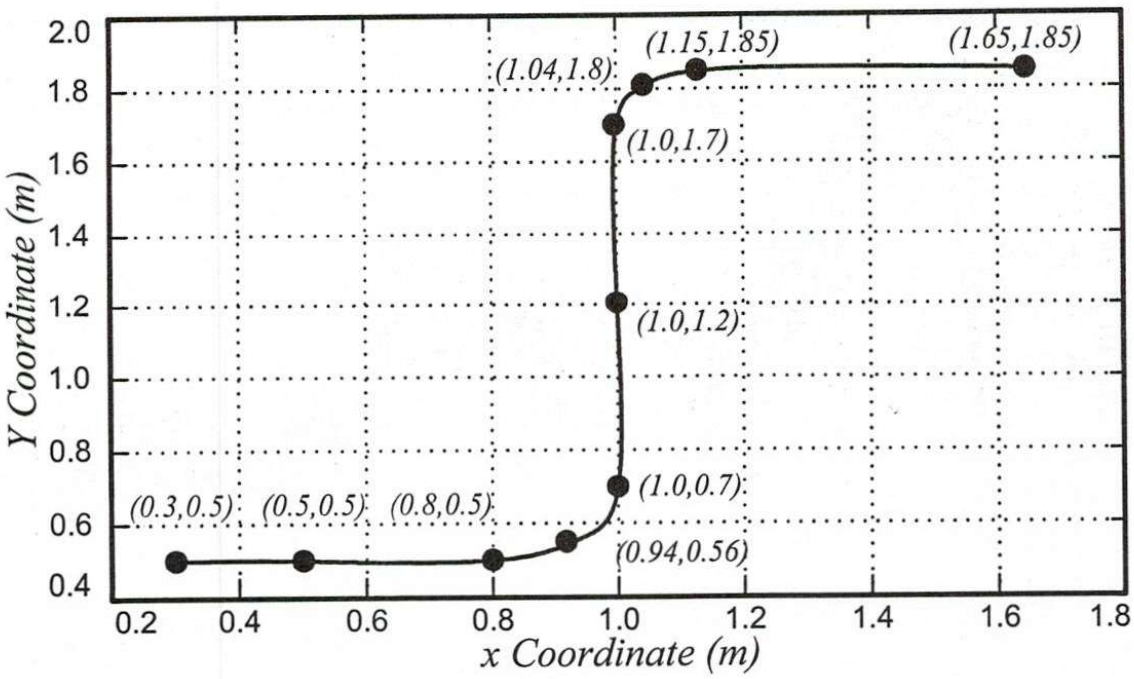

Fig 30. Reference trajectory for the experiment

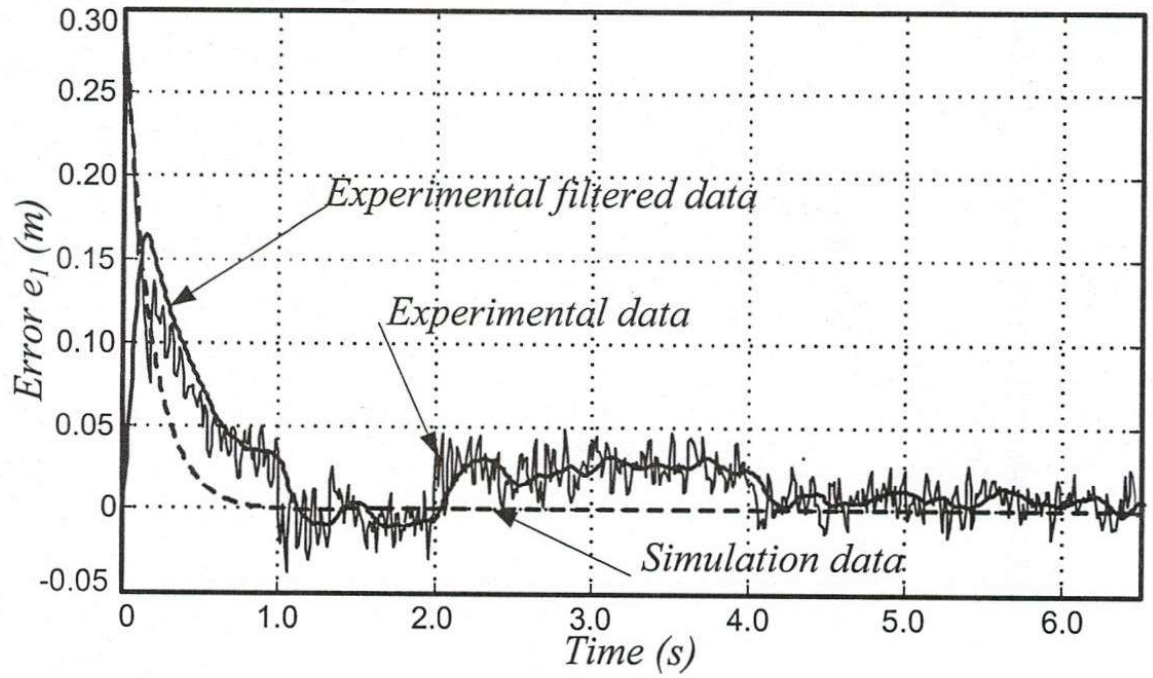

Fig 31. Experimental error e_1

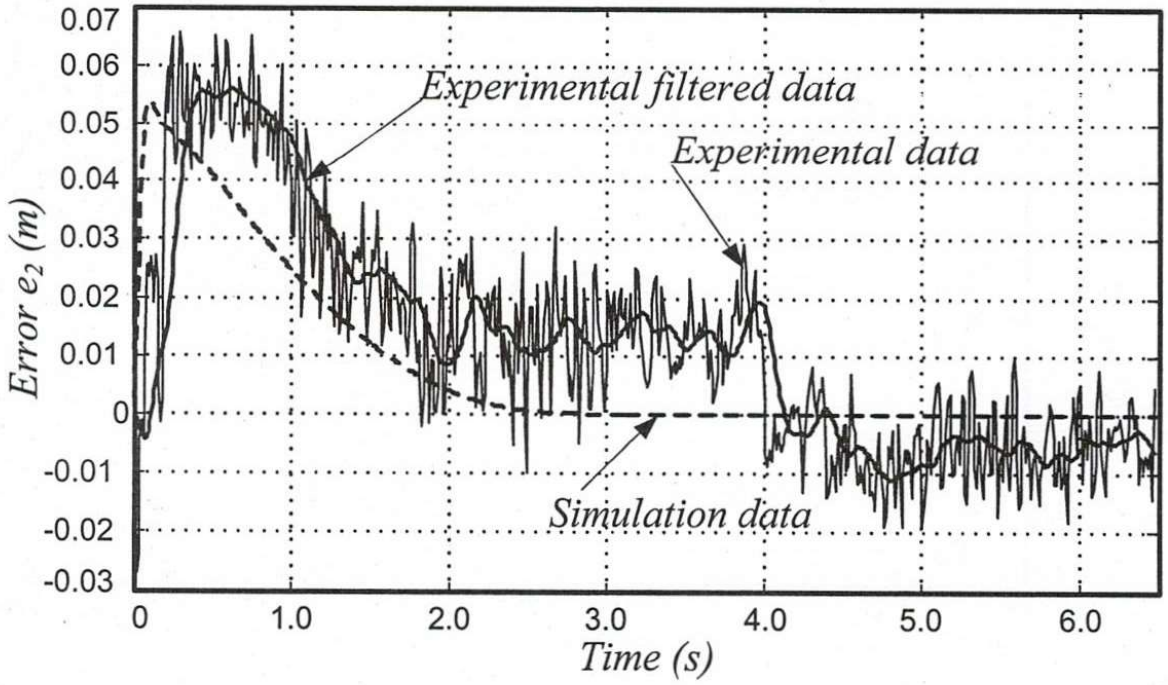

Fig 32. Experimental error e_2

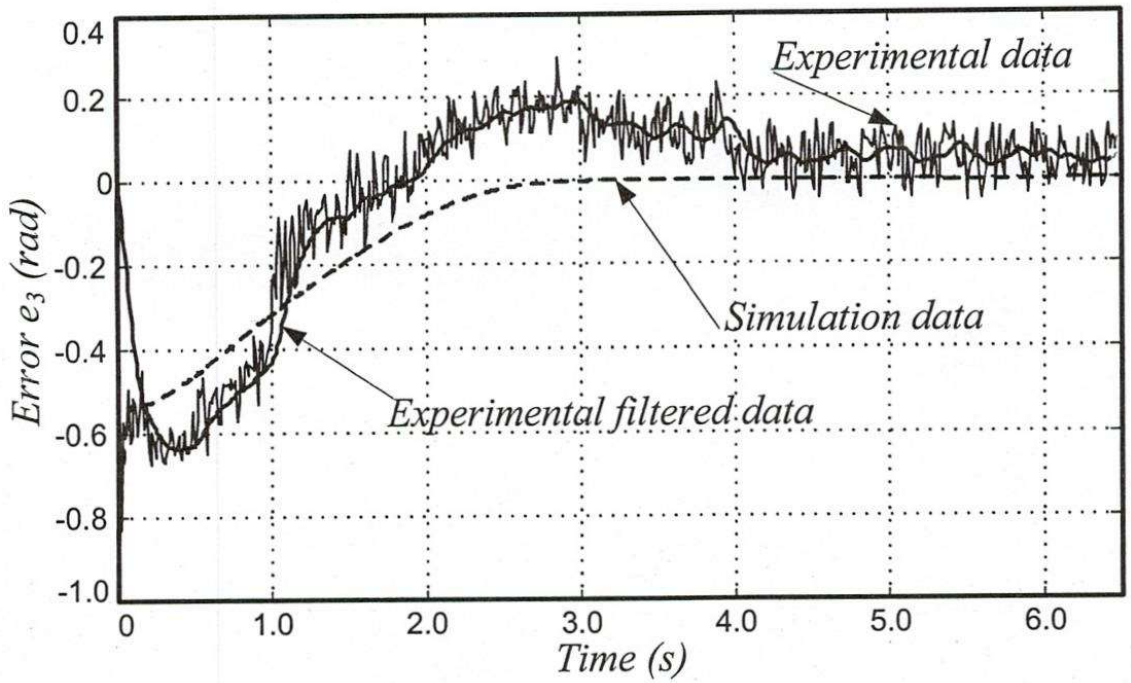

Fig 33. Experimental error e_3

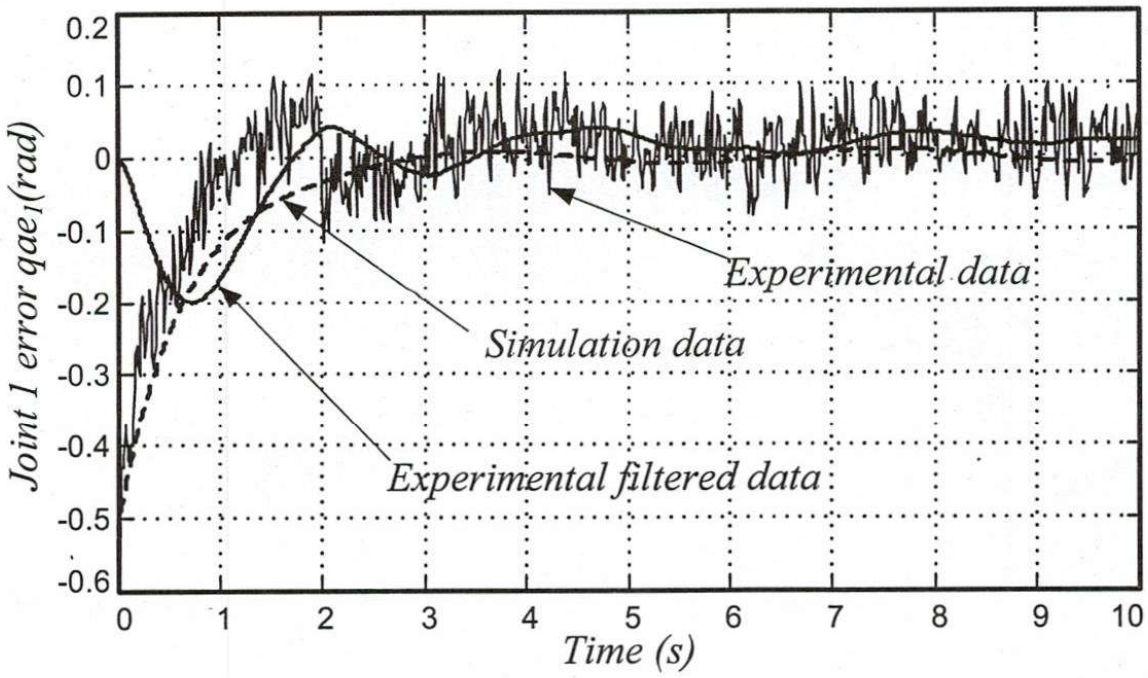

Fig 34. Experimental error of joint 1

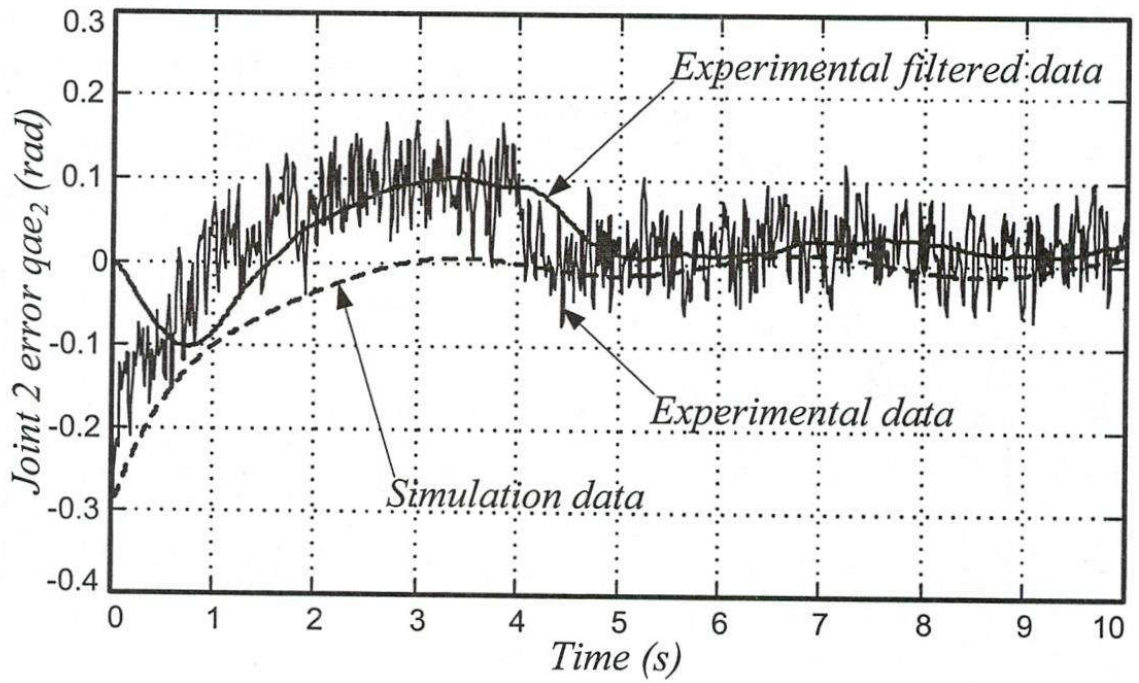

Fig 35. Experimental error of joint 2

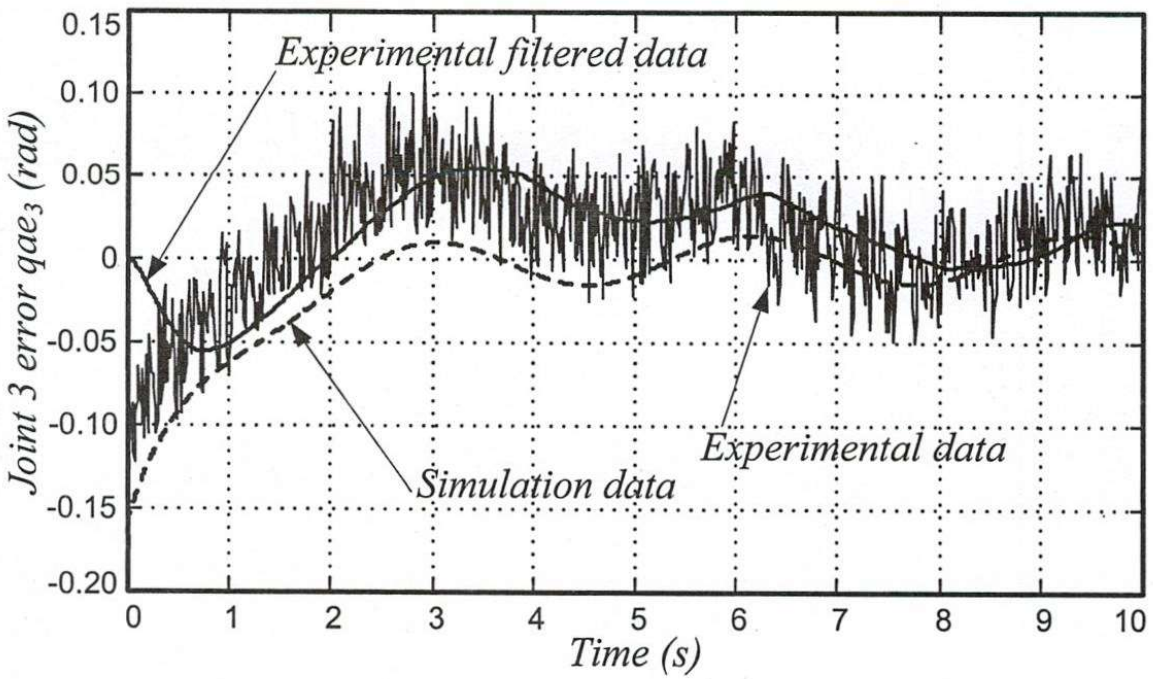

Fig 36. Experimental error of joint 3

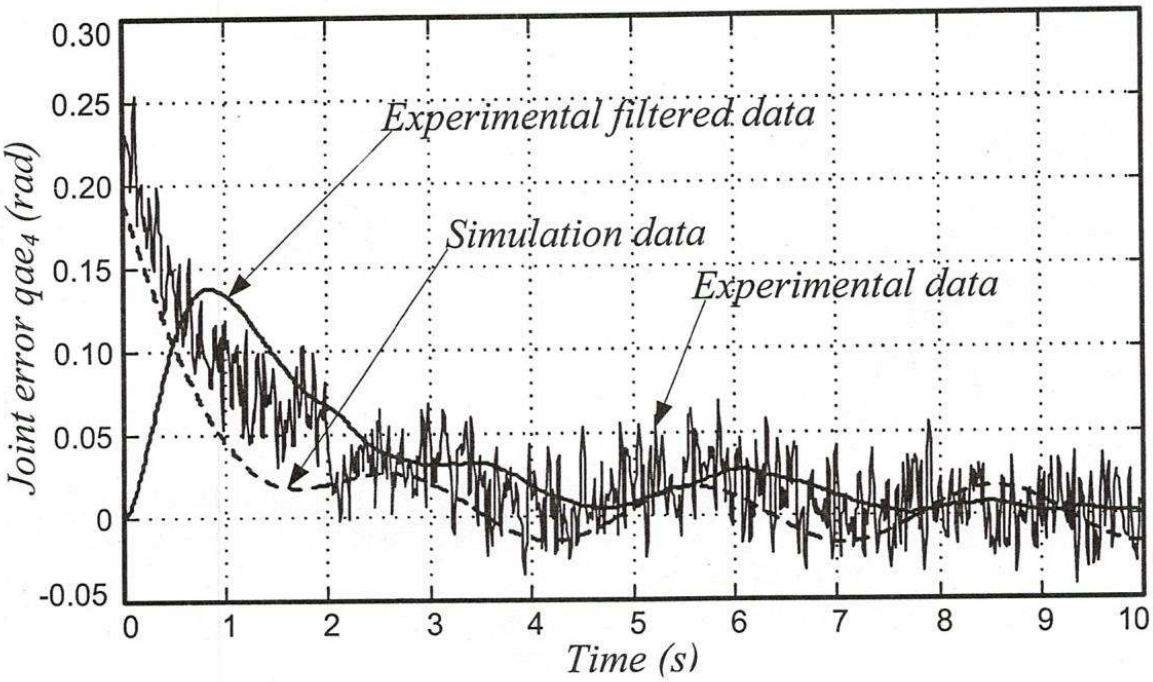

Fig 37. Experimental error of joint 4

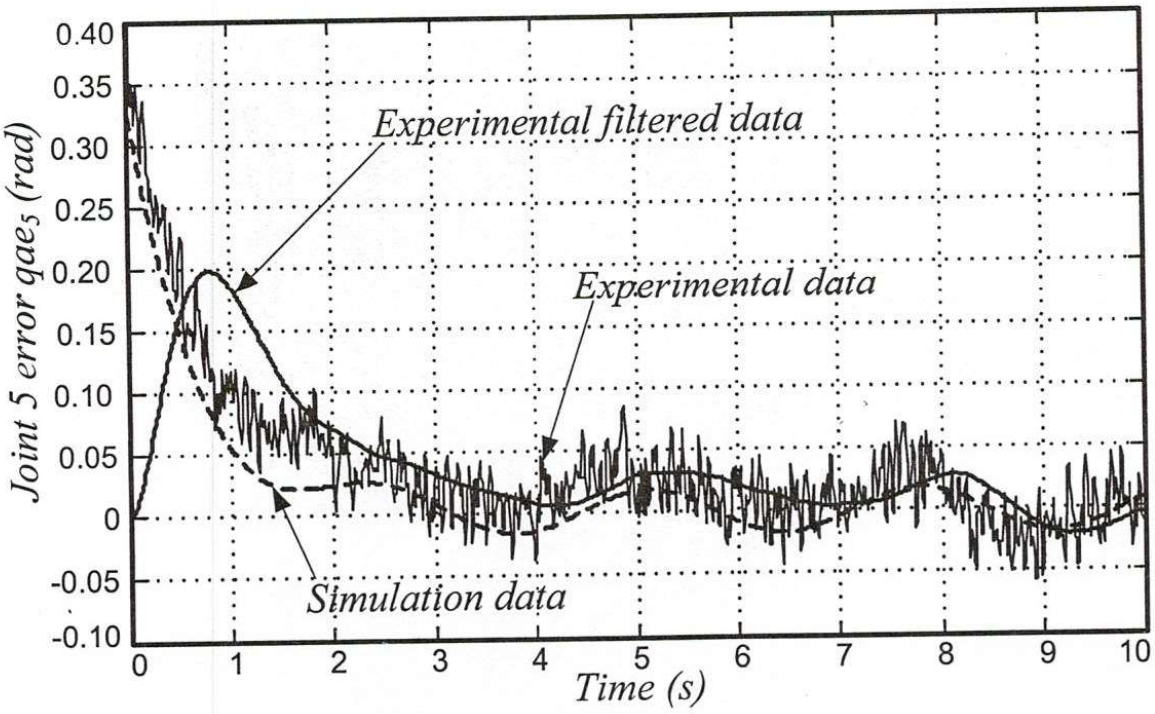

Fig 38. Experimental error of joint 5

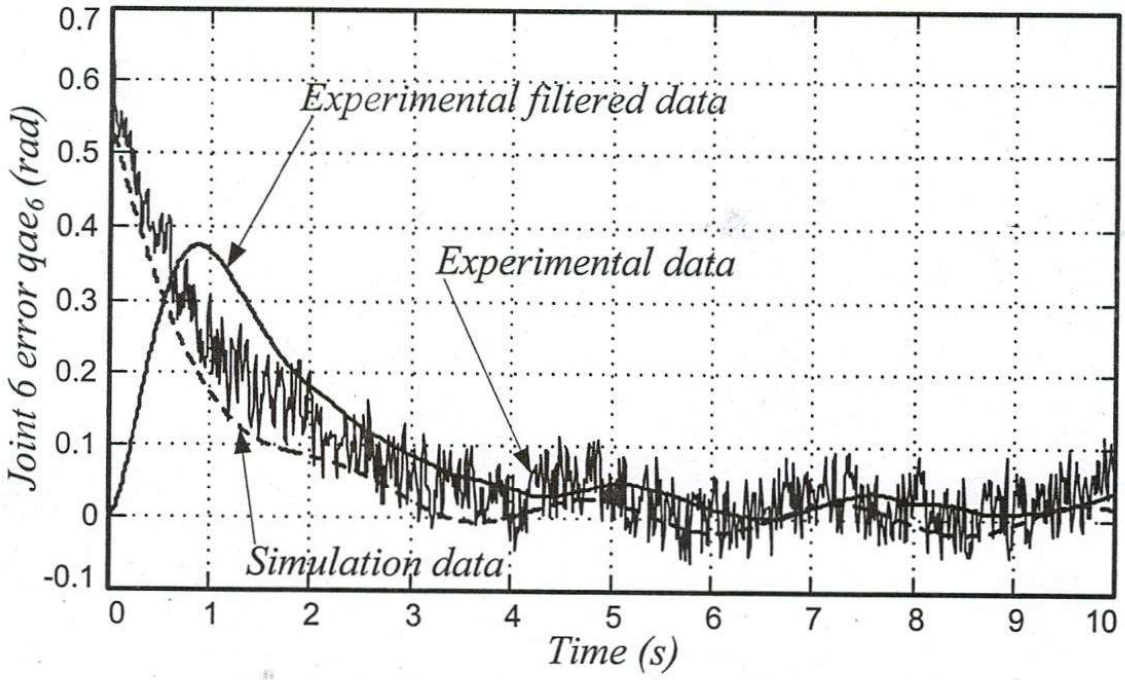

Fig 39. Experimental error of joint 6

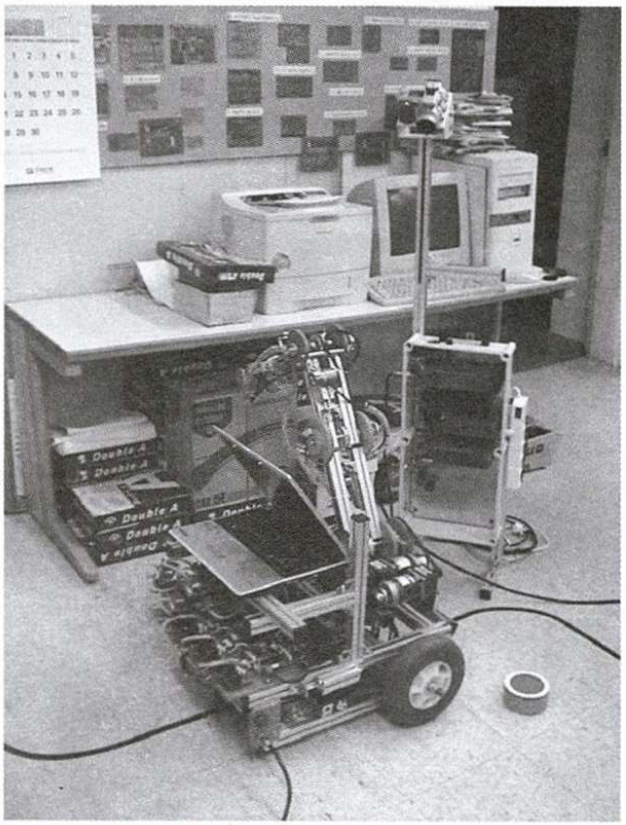

Fig 40. The experimental test bed

6. CONCLUSIONS

The robust controller was designed for the mobile manipulator to study on the dynamic behavior of such the combined system. The mobile manipulator is considered in terms of dynamic model. The tracking errors are defined, and the robust controller is designed for both the mobile platform and the manipulator to guarantee that the tracking errors go to zero asymptotically without the knowledge about system parameters and the external disturbance. The mobile robot and the manipulator can track the curved line at the bounded desired velocity. The simulation and the experimental results show that the controller is possible to implement in the practical field.

BỘ ĐIỀU KHIỂN THÍCH NGHI BỀN VỮNG CHO TAY MÁY DI ĐỘNG

Chung Tấn Lâm[(1)], Sang Bong Kim[(2)]
(1) PTN Trọng điểm Quốc gia Điều khiển số & Kỹ thuật hệ thống, ĐHQG-HCM
(2) Đại học Quốc gia Pukyong, Hàn Quốc

TÓM TẮT: *Trong bài báo này, điều khiển bền vững được thiết kế để điều khiển một tay máy đặt trên một robot di động dạng 2 bánh xe để quan sát hành vi động lực học của toàn bộ hệ thống. Khi đó, ta tìm phương trình động lực học của tay máy di động này có xét đến các tham số chưa xác định, nhiễu tác động, và tác động tương hỗ giữa chuyển động của robot di động và tay máy; sau đó, bộ điều khiển bền vững được thiết kế để bù trừ sự không xác định và nhiễu dựa vào quỹ đạo chuyển động mong muốn và thông tin từ cảm biến tại khớp và trên robot di động. Hệ thống điều khiển của hệ thống cũng được phát triển bao gồm sự kết hợp máy tính và bộ điều khiển dựa trên nền vi điều khiển PIC dùng truyền thông USB-CAN để đáp ứng yêu cầu hiệu suất điều khiển của toàn bộ hệ thống. Bài báo trình bày các kết quả mô phỏng và thực nghiệm để minh họa khả năng điều khiển của bộ điều khiển.*

Từ khóa: *robust adaptive controller, mobile manipulator*

REFERENCES

[1]. T. H. Bui, T. T. Nguyen, T. L. Chung, and Kim Sang Bong, "A Simple Nonlinear Control of a Two-Wheeled Welding Mobile Robot," *KIEE International Journal of Control, Automation*, and Systems, Vol. 1, No. 1, 2003, pp. 35-42.

[2]. R. Fierro and F.L. Lewis, "Control of a Non-holonomic Mobile Robot: Backstepping Kinematics into Dynamics," *in Proceedings of IEEE Conference on Decision & Control*, 1995, pp. 3805-3810.

[3]. J. M. Yang, I.-H. Choi, and J. H. Kim, "Sliding Mode Motion Control of a Nonholonomic Wheeled Mobile Robot for Trajectory Tracking," *in Proceedings of the IEEE Conference on Robotics & Automation*, 1998, pp. 2983-2988.

[4]. T. Fukao, H. Nakagawa and N. Adachi, 2000, "Adaptive Tracking Control of a Nonholonomic Mobile Robot," *IEEE Transaction on Robotics and Automation*, Vol. 16, No. 5, 2000, pp. 609-615.

[5]. D. K. Chwa, J. H. Seo, P. Kim, and J. Y. Choi, "Sliding Mode Tracking Control of Nonholonomic Wheeled Mobile Robots," *in Proceedings of the American Control Conference Anchorage*, 2002, pp. 3991-3996.

[6]. J. M. Yang and J. H. Kim, "Sliding Mode Motion Control of Nonholonomic Mobile Robots," *IEEE Transaction on Robotics and Automation*, Vol. 15, No. 3, 1999, pp. 578-587.

[7]. M. S. Kim and J. H. Shin, and J. J. Lee, "Design of a Robust Adaptive Controller for a Mobile Robot," *in Proceedings of the IEEE/RSJ International Conference on Intelligent Robots and Systems*, 2000, pp. 1816-1821.

[8]. M. V. Spong and M. Vidyasagar, Robot Dynamics and Control, John Wiley & Son Inc., New York, 1989.

[9]. M. W. Spong and M. Vidyasagar, "Robust Nonlinear Control of Robot Manipulators," *Proceedings of the 24th IEEE International Conference on Decision and Control*, 1985

[10]. M. Corless and G. Leitmann, "Continuous State Feedback Guaranteeing Uniform Ultimate Boundedness for Uncertain Dynamic System," *IEEE Transactions on Automatic Control*, Vol. 26, pp. 1139-1144, 1981.

[11]. S. Lin and A. A. Goldenberg, "Robust Damping Control of Mobile Manipulators," *IEEE Transactions on System, Man and Cybernetics*, Vol. 32, No.1, pp. 126 - 132, 2002.